

Robust Closed-Form Control for MIMO Nonlinear Systems under Conflicting Time-Varying Hard and Soft Constraints*

(extended version)

Farhad Mehdifar^a, Charalampos P. Bechlioulis^b, Dimos V. Dimarogonas^a

^a*Division of Decision and Control Systems, KTH Royal Institute of Technology, Stockholm, Sweden*

^b*Department of Electrical and Computer Engineering, University of Patras, Patra, Greece*

Abstract

This paper introduces a novel robust closed-form control law to handle time-varying hard and soft constraints in uncertain high-relative-degree nonlinear MIMO systems. These constraints represent spatiotemporal specifications in mechanical systems' operational space, with hard constraints ensuring safety-critical requirements and soft constraints encoding performance or task objectives. Initially, all constraints are consolidated into two separate scalar time-varying hard and soft constraint functions, whose positive level sets define feasible regions. A closed-form control law is developed to enforce these constraints using appropriately designed reciprocal barriers and nonlinear transformation functions. When conflicts between hard and soft constraints arise, the control law prioritizes hard constraints by virtually relaxing soft constraints via a dynamic relaxation law. Notably, the proposed control law maintains low complexity by avoiding approximation schemes for coping with system uncertainties. Simulation results confirm the effectiveness of the proposed method.

Keywords: Time-Varying Hard and Soft Constraints, Uncertain MIMO Nonlinear System, Low-Complexity Control, Reciprocal Barrier Functions

1. Introduction

In recent years, advances in science and technology have profoundly influenced control system design, shifting the focus beyond traditional objectives like stability and accuracy toward explicitly enforcing transient performance and safety requirements. These specifications are typically imposed by introducing (often time-varying) constraints in controller design for practical nonlinear systems, where violations may cause performance degradation, system damage, or safety hazards. To address this, a range of control strategies has been developed to guarantee desired performance and/or prevent unsafe behavior, including Model Predictive Control (MPC) [1], Reference Governors (RGs) [2, 3], Control Barrier Functions (CBFs) [4], Barrier Lyapunov Functions (BLFs) [5, 6], Funnel Control (FC) [7], and Prescribed Performance Control (PPC) [8]. Each approach offers distinct strengths and limitations in enforcing performance and safety constraints.

Among the aforementioned strategies, BLFs, FC, and PPC provide closed-form and robust designs for uncertain nonlinear systems, enforcing time-varying funnel-type constraints, $\underline{\rho}_i(t) < e_i = x_i - x_i^d(t) < \bar{\rho}_i(t)$, on independent

tracking errors, where x_i denotes independent state variables and $x_i^d(t)$ the desired trajectories. By properly designing the time-varying boundaries $\bar{\rho}_i(t) > \underline{\rho}_i(t)$, one can prescribe desired transient and steady-state performance of tracking errors while satisfying certain classes of safety requirements. To achieve this, time-varying BLFs are constructed such that, as tracking errors approach the prescribed boundaries, the BLFs diverge to infinity, ensuring that system states respect the constraints [6, 9]. PPC, in contrast, employs an error transformation that maps the original constrained system into an unconstrained one, where establishing uniform ultimate boundedness of the transformed system provides a necessary and sufficient solution [8, 10]. Notably, the PPC transformation implicitly induces a constructive time-varying BLF in its design. FC, in contrast, generalizes adaptive high-gain control by replacing the monotonically increasing gain with a time-varying, state-dependent function that enforces funnel constraints [11, 12].

Despite notable progress in BLF-, FC-, and PPC-based designs, existing frameworks face two structural limitations when addressing general time-varying constraints. First, they are largely tailored to collections of decoupled, funnel-type constraints, which limits their applicability to richer set representations and hinders seamless deployment across diverse scenarios. Second, systematically handling potentially conflicting time-varying hard

*This work is supported by ERC CoG LEAFHOUND, the KAW foundation, and the Swedish Research Council (VR).

Email addresses: mehdifar@kth.se (Farhad Mehdifar), chmpech1@upatras.gr (Charalampos P. Bechlioulis), dimos@kth.se (Dimos V. Dimarogonas)

and soft constraints within these methodologies remains largely unresolved.

This paper presents a tractable, closed-form robust control law that manages the interplay between explicitly defined and potentially conflicting time-varying hard (safety) and soft (performance) constraints. Unlike optimization-based synthesis (e.g., MPC and CBFs), which typically uses slack variables to relax soft constraints in favor of hard ones [13, 14], deriving robust closed-form controllers that enforce hard constraints while accommodating soft ones is more difficult. We also note that hard and soft constraints can arise implicitly, for example, having hard control input limits and soft performance specifications, or from conflicts between time-varying (soft) position and (hard) velocity bounds in mechanical systems, see for example [15, 16, 17, 18, 19], which are topics outside the scope of this article.

Regarding the constraint classes considered by BLF, FC, and PPC-based methods, recent studies mainly focus on integrating diverse time-varying boundary functions into funnel constraints, including asymmetric [9], fixed/finite-time [20, 21], and tunnel [22, 23] bounds. A well-known limitation of BLF- and PPC-based designs is the need for initial satisfaction of funnel constraints, which requires knowledge of the system's initial condition to tune the bound values. To address this, many works employ large initial funnel bounds [24], whereas deferred time-varying funnel constraints inherently remove dependence on the initial condition [25, 26]. This approach has further been extended to irregular, intermittently active output funnel constraints in [27, 28, 29].

Collectively, these results address only funnel-type constraints, typically imposed on independent states or error signals that remain decoupled, so satisfying one does not affect the others. Consequently, BLF/FC/PPC formulations yield time-varying box constraints in the output/error space [30, 10, 9]. Our prior work [31, 32] overcame this by unifying multiple classes of time-varying constraints (beyond funnels) into a single scalar, time-varying constraint function whose positive level set defines the feasible region, and by proposing a robust closed-form control law that guarantees constraint satisfaction.

Concerning management of time-varying hard and soft constraints, most BLF-, FC-, and PPC-based results treat tracking-performance (funnel) constraints as inviolable. This can still permit satisfaction of certain hard (safety) constraints alongside tracking-error specifications when the hard constraints can be expressed in terms of system errors and are always compatible with the performance bounds. This approach is common, e.g., in multi-agent formation control, where performance bounds on formation errors are designed so that their satisfaction also enforces hard constraints such as connectivity maintenance, inter-agent collision avoidance, and visibility (field-of-view) constraints [33, 34, 35, 36, 37].

For potentially conflicting time-varying hard and soft constraints, only a few results exist. In particular, [38]

studies trajectory tracking (as a soft constraint) under irregular, intermittent funnel-type hard constraints and proposes smooth modification of the desired trajectory to comply with the hard specifications. The work in [39] explicitly considers hard and soft funnel-type constraints and provides a constraint-consistent online funnel-planning scheme that respects hard constraints at all times and satisfies the soft ones when possible. This framework has since been extended to handle reach-avoid-stay specifications [40] and to control flexible beam systems [41]. A BLF-based cooperative tracking-in-information design for marine vehicles is proposed in [42], treating inter-agent connectivity maintenance and collision avoidance as hard specifications and non-negativity of surge velocity as a soft requirement. Authors in [43] propose flexible performance bounds for trajectory tracking of surface-vehicles with moving-obstacle avoidance, which dynamically relaxes tracking performance when the collision-avoidance module activates; this strategy is also extended to formation tracking problems in [44]. Although these works provide closed-form robust control for hard and soft constraints, they either remain restricted to funnel-type specifications or are tailored to particular applications, limiting straightforward generalization.

Motivated by these gaps and limitations, this paper presents a novel robust closed-form control law for uncertain high-relative-degree nonlinear MIMO systems subject to a generalized class of time-varying hard and soft constraints. In our framework, constraints are explicitly defined and can model coupled spatiotemporal specifications in a mechanical system's operational space. All constraints are encoded into two scalar functions, one hard and one soft, whose positive level sets define the feasible regions. Using suitably designed reciprocal barrier functions, we derive robust closed-form velocity-level control laws that enforce both classes of constraints. In the presence of conflicts, the method prioritizes hard constraints by virtually relaxing the soft ones through a dynamic relaxation scheme. Through tailored nonlinear transformations and a low-complexity backstepping-like design, we then lift the velocity-level law to actual control inputs without relying on approximation or estimation of uncertainties. Moreover, embedding shifting functions decouples controller tuning from the system's initial condition, strengthening stability guarantees from semi-global to global. While our earlier work [32] addressed generalized time-varying constraints, it did not account for the interaction between hard and soft constraints. Similarly, the results in [39] are restricted to cases where both hard and soft sets are intersections of decoupled time-varying funnel-type constraints, yielding only time-varying hard and soft box sets. In contrast, building on the ideas in [32], this work introduces a new control design methodology capable of handling generalized time-varying hard and soft constraint sets with arbitrary shapes.

Notations: \mathbb{N} and \mathbb{R} denote the sets of natural and real numbers, respectively. $\mathbb{R}_{\geq 0}$, $\mathbb{R}_{> 0}$, and $\mathbb{R}_{\leq 0}$ denote

non-negative, positive, and non-positive reals. \mathbb{R}^n is the n -dimensional real vector space. Bold lowercase symbols represent vectors or vector-valued functions, while bold uppercase denote matrices; non-bold symbols refer to scalars or scalar-valued functions. For instance, $\mathbf{a} \in \mathbb{R}^n$ is an $n \times 1$ column vector, \mathbf{a}^\top its transpose, and $\|\mathbf{a}\|$ its Euclidean norm. The column-concatenation operator is $\text{col}(\mathbf{a}_i) := [\mathbf{a}_1^\top, \dots, \mathbf{a}_m^\top]^\top \in \mathbb{R}^{mn}$, where $\mathbf{a}_i \in \mathbb{R}^n$, $i \in 1, \dots, m$. The set of real $n \times m$ matrices is $\mathbb{R}^{n \times m}$. For $\mathbf{A} \in \mathbb{R}^{n \times m}$, \mathbf{A}^\top is the transpose and $\|\mathbf{A}\|$ the induced norm. The absolute value of a scalar is $|\cdot|$. The n -dimensional identity matrix is $\mathbf{I}_n \in \mathbb{R}^{n \times n}$ and $\mathbf{0}_n \in \mathbb{R}^n$ is the zero vector. The operator $\text{diag}(\cdot)$ forms a diagonal matrix. The closure of an open set Ω is $\text{cl}(\Omega)$. The class of n -times continuously differentiable functions is \mathcal{C}^n , and \mathcal{L}_∞ denotes essentially bounded measurable functions. The index set $\mathbb{I}_i^j := i, \dots, j$ is defined for $i, j \in \mathbb{N}$ with $i < j$.

2. Problem Formulation

Consider the following class of high-relative-degree MIMO nonlinear systems:

$$\begin{aligned}\dot{\mathbf{x}}_i &= \mathbf{f}_i(t, \bar{\mathbf{x}}_i) + \mathbf{G}_i(t, \bar{\mathbf{x}}_i)\mathbf{x}_{i+1}, \quad i \in \mathbb{I}_1^{r-1} \\ \dot{\mathbf{x}}_r &= \mathbf{f}_r(t, \bar{\mathbf{x}}_r) + \mathbf{G}_r(t, \bar{\mathbf{x}}_r)\mathbf{u},\end{aligned}\quad (1)$$

where $\mathbf{x}_i := [x_{i,1}, x_{i,2}, \dots, x_{i,n}]^\top \in \mathbb{R}^n$, $\bar{\mathbf{x}}_i := [\mathbf{x}_1^\top, \dots, \mathbf{x}_i^\top]^\top \in \mathbb{R}^{ni}$, $i \in \mathbb{I}_1^r$, and $r \in \mathbb{N}$. Moreover, $\mathbf{x} := \bar{\mathbf{x}}_r \in \mathbb{R}^{nr}$ is the state vector, which is available for measurement and $\mathbf{u} \in \mathbb{R}^n$ is the control input of the system. Furthermore, $\mathbf{f}_i : \mathbb{R}_{\geq 0} \times \mathbb{R}^{ni} \rightarrow \mathbb{R}^n$, and $\mathbf{G}_i : \mathbb{R}_{\geq 0} \times \mathbb{R}^{ni} \rightarrow \mathbb{R}^{n \times n}$, $i \in \mathbb{I}_1^r$ are vector fields that are piece-wise continuous in t and locally Lipschitz continuous in $\bar{\mathbf{x}}_i$ for each $t \in \mathbb{R}_{\geq 0}$. Let $\mathbf{x}(t; \mathbf{x}(0), \mathbf{u})$ signify the solution of (1) under the initial condition $\mathbf{x}(0)$ and control input \mathbf{u} . By $\mathbf{x}_1(t; \mathbf{x}(0)) := \mathbf{x}_1(t; \mathbf{x}(0), \mathbf{u})$ we refer to the partial solution of the closed-loop system (1) with respect to the state variables \mathbf{x}_1 .

Assumption 1. The matrix $\mathbf{G}_1(t, \mathbf{x}_1)$ is known and uniformly sign-definite $\forall t \geq 0$ and $\forall \mathbf{x}_1 \in \mathbb{R}^n$. Without loss of generality, in this work we assume that $\mathbf{G}_1(t, \mathbf{x}_1)$ is positive definite. Moreover, we assume that $\mathbf{f}_i(\cdot, \cdot), \forall i \in \mathbb{I}_1^r$, and $\mathbf{G}_i(\cdot, \cdot), \forall i \in \mathbb{I}_2^r$, are unknown.

Assumption 2. All elements of the maps $\mathbf{f}_i : \mathbb{R}_{\geq 0} \times \mathbb{R}^{ni} \rightarrow \mathbb{R}^n$, and $\mathbf{G}_i : \mathbb{R}_{\geq 0} \times \mathbb{R}^{ni} \rightarrow \mathbb{R}^{n \times n}$, $i \in \mathbb{I}_1^r$, are bounded for each fixed $\bar{\mathbf{x}}_i \in \mathbb{R}^{ni}$ and for all $t \geq 0$. In other words, there exist locally Lipschitz functions $\bar{f}_i : \mathbb{R}^{ni} \rightarrow \mathbb{R}$ and $\bar{g}_i : \mathbb{R}^{ni} \rightarrow \mathbb{R}$, $i \in \mathbb{I}_1^r$, with unknown analytical expressions such that $\|\mathbf{f}_i(t, \bar{\mathbf{x}}_i)\| \leq \bar{f}_i(\bar{\mathbf{x}}_i)$ and $\|\mathbf{G}_i(t, \bar{\mathbf{x}}_i)\| \leq \bar{g}_i(\bar{\mathbf{x}}_i)$, for all $t \geq 0$ and all $\bar{\mathbf{x}}_i \in \mathbb{R}^{ni}$.

Assumption 3. The matrices $\tilde{\mathbf{G}}_i(t, \bar{\mathbf{x}}_i) := \frac{1}{2}(\mathbf{G}_i^\top + \mathbf{G}_i)$, $i \in \mathbb{I}_2^r$, are uniformly sign-definite with known signs $\forall t \geq 0$ and $\forall \bar{\mathbf{x}}_i \in \mathbb{R}^{ni}$. Without loss of generality, we assume that all $\tilde{\mathbf{G}}_i(t, \bar{\mathbf{x}}_i)$ are positive definite, implying the existence of unknown strictly positive constants $\lambda_i > 0$, $i \in \mathbb{I}_1^r$, such that $\lambda_{\min}(\tilde{\mathbf{G}}_i(t, \bar{\mathbf{x}}_i)) \geq \lambda_i > 0$, $\forall t \geq 0$ and $\forall \bar{\mathbf{x}}_i \in \mathbb{R}^{ni}$.

As stated in Assumption 1, $\mathbf{G}_1(t, \mathbf{x}_1)$ is a known positive definite matrix. However, this is rarely restrictive in practice, as most common mechanical systems satisfy $\mathbf{G}_1(t, \mathbf{x}_1) = \mathbf{I}_n$. Assumption 2 suggests that while the unknown elements of $\mathbf{f}_i(t, \bar{\mathbf{x}}_i)$ and $\mathbf{G}_i(t, \bar{\mathbf{x}}_i)$, $i \in \mathbb{I}_1^r$, can grow arbitrarily large due to variations in $\bar{\mathbf{x}}_i$, they cannot do so as a result of increase in t . Furthermore, Assumption 3, together with the positive definiteness of $\mathbf{G}_1(t, \mathbf{x}_1)$, establishes a global controllability condition for (1).

Let the dynamical system (1) be subject to the following generalized class of time-varying constraints with respect to \mathbf{x}_1 states

$$\psi_{h_j}(t, \mathbf{x}_1) > 0, \quad j \in \mathbb{I}_1^{m_s}, \quad (2a)$$

$$\psi_{s_j}(t, \mathbf{x}_1) > 0, \quad j \in \mathbb{I}_1^{m_h}, \quad (2b)$$

where $m_s, m_h \in \mathbb{N}$, and $\psi_{h_j}, \psi_{s_j} : \mathbb{R}_{\geq 0} \times \mathbb{R}^n \rightarrow \mathbb{R}$ are continuously differentiable functions in their arguments representing hard and soft inequality-type constraints, respectively. In practical mechanical systems modeled by (1), the state partition \mathbf{x}_1 typically represents spatial coordinates (positions). As a result, the time-varying hard and soft constraints in (2) naturally encode spatiotemporal (space and time) specifications.

We make the following regularity assumptions for $\psi_{h_j}(\cdot, \cdot)$ and $\psi_{s_j}(\cdot, \cdot)$.

Assumption 4. Functions $\psi_{\star_j}(\cdot, \cdot), j \in \mathbb{I}_1^{m_\star}, \star \in \{h, s\}$, are bounded for each fixed $\mathbf{x}_1 \in \mathbb{R}^n$ and for all $t \geq 0$, i.e., there exist continuous functions $\bar{\psi}_{\star_j} : \mathbb{R}^n \rightarrow \mathbb{R}$, such that $|\psi_{\star_j}(t, \mathbf{x}_1)| \leq \bar{\psi}_{\star_j}(\mathbf{x}_1)$, for all $t \geq 0$ and all $\mathbf{x}_1 \in \mathbb{R}^n$.

Assumption 5. There exist continuous functions $\kappa_{\star_j} : \mathbb{R}^n \rightarrow \mathbb{R}$ and $\iota_{\star_j} : \mathbb{R}^n \rightarrow \mathbb{R}$, $j \in \mathbb{I}_1^{m_\star}, \star \in \{h, s\}$, such that $|\frac{\partial \psi_{\star_j}^j(t, \mathbf{x}_1)}{\partial \mathbf{x}_1}| \leq \kappa_{\star_j}(\mathbf{x}_1)$ and $|\frac{\partial \psi_{\star_j}^j(t, \mathbf{x}_1)}{\partial t}| \leq \iota_{\star_j}(\mathbf{x}_1)$, for all $t \geq 0$ and all $\mathbf{x}_1 \in \mathbb{R}^n$.

Since the constraint functions in (2) are known, the upper bounds introduced in Assumptions 4 and 5 are likewise known. These bounds are needed exclusively for the stability analysis and do not influence the controller design. In particular, their existence ensures that, for any fixed \mathbf{x}_1 , the constraint functions in (2) and their derivatives remain bounded for all time.

Define the hard and soft constraint sets as follows:

$$\bar{\Omega}_h(t) := \{\mathbf{x}_1 \in \mathbb{R}^n \mid \psi_{h_j}(t, \mathbf{x}_1) > 0, \forall j \in \mathbb{I}_1^{m_h}\}, \quad (3a)$$

$$\bar{\Omega}_s(t) := \{\mathbf{x}_1 \in \mathbb{R}^n \mid \psi_{s_j}(t, \mathbf{x}_1) > 0, \forall j \in \mathbb{I}_1^{m_s}\}. \quad (3b)$$

Objective: In this article, we aim to design a closed-form, low-complexity robust continuous control law $\mathbf{u}(t, \mathbf{x})$ for (1) that ensures $\mathbf{x}_1(t; \mathbf{x}(0))$ adheres to the time-varying hard constraints (2a) at all times (i.e., $\mathbf{x}_1(t; \mathbf{x}(0)) \in \bar{\Omega}_h(t), \forall t \geq 0$). Additionally, the time-varying soft constraints (2b) are required to be satisfied only when they are compatible with the hard constraints (i.e., $\bar{\Omega}_h(t) \cap \bar{\Omega}_s(t) \neq \emptyset$). Specifically, in the absence of incompatibilities, if the soft constraints are not initially met, our goal is to achieve their satisfaction $\forall t \geq T > 0$, where T is a user-defined finite time.

3. Main Results

In this section, we first introduce smooth consolidated hard and soft constraint functions, whose positive level sets provide smooth inner-approximations of the hard and soft constrained sets in (3), respectively. Next, we propose a low-complexity control design strategy to achieve the stated objectives. Finally, we summarize the main results of this article in Theorem 1 and Corollary 1.

3.1. Smooth Consolidated Hard and Soft Constraint Functions

Note that hard and soft constraints in (2a) and (2b) are satisfied whenever

$$\bar{\alpha}_h(t, \mathbf{x}_1) := \min\{\psi_{h_1}(t, \mathbf{x}_1), \dots, \psi_{h_{m_h}}(t, \mathbf{x}_1)\} > 0, \quad (4a)$$

$$\bar{\alpha}_s(t, \mathbf{x}_1) := \min\{\psi_{s_1}(t, \mathbf{x}_1), \dots, \psi_{s_{m_s}}(t, \mathbf{x}_1)\} > 0, \quad (4b)$$

hold, respectively. Therefore, hard and soft constrained sets in (3) can be equivalently expressed as $\bar{\Omega}_*(t) = \{\mathbf{x}_1 \in \mathbb{R}^n \mid \bar{\alpha}_*(t, \mathbf{x}_1) > 0\}$, where $* \in \{h, s\}$. In general, $\bar{\alpha}_h(\cdot, \cdot)$ and $\bar{\alpha}_s(\cdot, \cdot)$ are continuous yet nonsmooth in \mathbf{x}_1 . Using the Log-Sum-Exp function, we introduce *smooth consolidated hard and soft constraint functions* as follows:

$$\alpha_h(t, \mathbf{x}_1) := -\frac{1}{\nu} \ln \left(\sum_{j=1}^{m_h} e^{-\nu \psi_{h_j}(t, \mathbf{x}_1)} \right) \quad (5a)$$

$$\alpha_s(t, \mathbf{x}_1) := -\frac{1}{\nu} \ln \left(\sum_{j=1}^{m_s} e^{-\nu \psi_{s_j}(t, \mathbf{x}_1)} \right) \quad (5b)$$

where $\nu > 0$ is a tuning coefficient whose larger values gives a closer (under) approximation (i.e., $\alpha_*(t, \mathbf{x}_1) \rightarrow \bar{\alpha}_*(t, \mathbf{x}_1)$ as $\nu \rightarrow \infty$, $* \in \{h, s\}$). In particular, it is known that $\alpha_*(t, \mathbf{x}_1) \leq \bar{\alpha}_*(t, \mathbf{x}_1) \leq \alpha_*(t, \mathbf{x}_1) + \frac{1}{\nu} \ln(m_*)$, $* \in \{h, s\}$ [45]. Clearly, ensuring $\alpha_*(t, \mathbf{x}_1) > 0$ guarantees $\bar{\alpha}_*(t, \mathbf{x}_1) > 0$, $* \in \{h, s\}$, and thus the satisfaction of (2).

Define

$$\Omega_h(t) := \{\mathbf{x}_1 \in \mathbb{R}^n \mid \alpha_h(t, \mathbf{x}_1) > 0\} \subseteq \bar{\Omega}_h(t), \quad (6a)$$

$$\Omega_s(t) := \{\mathbf{x}_1 \in \mathbb{R}^n \mid \alpha_s(t, \mathbf{x}_1) > 0\} \subseteq \bar{\Omega}_s(t), \quad (6b)$$

which represent *smooth inner-approximations* of the hard and soft constrained sets in (3), respectively.

Assumption 6. Functions $-\bar{\alpha}_*(t, \mathbf{x}_1), * \in \{h, s\}$ are coercive (radially unbounded) in \mathbf{x}_1 and uniformly in t , i.e., $-\bar{\alpha}_*(t, \mathbf{x}_1) \rightarrow +\infty$ as $\|\mathbf{x}_1\| \rightarrow +\infty, \forall t \geq 0$.

The above assumption is both necessary and sufficient for the level curves of $\bar{\alpha}_*(t, \mathbf{x}_1), * \in \{h, s\}$ (and consequently $\alpha_*(t, \mathbf{x}_1)$) to be compact for all $t \geq 0$. Thus, Assumption 6 guarantees the boundedness of the hard and soft constrained sets in (3) (and their smooth inner approximations in (6)), thereby establishing a well-posedness condition for time-varying hard and soft constrained sets; see [32, Lemma 1].

From (4) (resp. (5)), Assumption 6 can be verified for either hard or soft constrained sets by checking if at least one of the functions $\psi_{\star_j}(t, \mathbf{x}_1), \star \in \{h, s\}$ in (2) approaches $-\infty$ as $\|\mathbf{x}_1\| \rightarrow +\infty$ (along any path in \mathbb{R}^n). As outlined in [32, Section III.A], this assumption can also be readily ensured by introducing auxiliary (hard or soft) constraints in the form of $\bar{\psi}_{\star_{\text{aux}}}(\mathbf{x}_1) := c_{\text{aux}} - \|\mathbf{x}_1\|^2, \star \in \{h, s\}$, where $c_{\text{aux}} > 0$ is a sufficiently large constant.

Note that Assumption 6 also guarantees the existence of at least one global maximizer for $\bar{\alpha}_h(t, \mathbf{x}_1)$ and $\bar{\alpha}_s(t, \mathbf{x}_1)$ (resp. for $\alpha_h(t, \mathbf{x}_1)$ and $\alpha_s(t, \mathbf{x}_1)$) for all $t \geq 0$, see [46, Proposition 2.9]. Accordingly, associated with the sets $\Omega_h(t)$ and $\Omega_s(t)$, we define $\alpha_h^*(t) := \max_{\mathbf{x}_1 \in \mathbb{R}^n} \alpha_h(t, \mathbf{x}_1)$ and $\alpha_s^*(t) := \max_{\mathbf{x}_1 \in \mathbb{R}^n} \alpha_s(t, \mathbf{x}_1)$ for each instant t . Clearly, $\alpha_h^*(t') > 0$ and $\alpha_s^*(t') > 0$ signify the feasibility of $\Omega_h(t)$ and $\Omega_s(t)$ in (6) at time $t = t'$, respectively.

Assumption 7. Each of the inner-approximated hard and soft constrained sets, i.e., $\Omega_h(t)$ and $\Omega_s(t)$, are nonempty (feasible) for all $t \geq 0$.

The above assumption ensures the existence of sufficiently small positive constants $\epsilon_h > 0$ and $\epsilon_s > 0$ such that $\alpha_h^*(t) \geq \epsilon_h > 0$ and $\alpha_s^*(t) \geq \epsilon_s > 0$ for all $t \geq 0$.

Assumption 8. The initial condition $\mathbf{x}(0)$ of the system (1) is such that $\alpha_h(0, \mathbf{x}_1(0)) > 0$, i.e., the hard constraints are satisfied at time $t = 0$.

Remark 1. Note that the feasibility of the inner-approximated hard and soft constrained sets $\Omega_h(t)$ and $\Omega_s(t)$ ensures the feasibility of $\bar{\Omega}_h(t)$ and $\bar{\Omega}_s(t)$ in (3). Furthermore, if the original time-varying hard and soft constrained sets $\bar{\Omega}_h(t)$ and $\bar{\Omega}_s(t)$ are tightly feasible (i.e., relatively small), one can always select a sufficiently large ν in (5) to ensure that Assumption 7 remains valid.

3.2. Hard and Soft Constraints Satisfaction Strategy

We begin with designing two scalar time-varying constraints for system (1), which, when they are satisfied, guarantee the hard constraints (2a) are met at all times and the soft constraints (2b) are met only when compatible with the hard constraints. In the next subsection, we propose a control law to enforce these time-varying constraints along the closed-loop system trajectories. Hereafter, for brevity, we refer to $\Omega_h(t)$ and $\Omega_s(t)$ in (6) as the time-varying hard and soft constrained sets (excluding the inner-approximation term) when there is no ambiguity.

Based on the alternative formulation of time-varying hard constraints in (6a), enforcing

$$0 < \alpha_h(t, \mathbf{x}_1), \quad \forall t \geq 0, \quad (7)$$

along trajectories of (1) guarantees that the hard constraints (2a) hold for all $t \geq 0$. Notice that, (7) is a feasible constraint at all times under Assumptions 7 and 8.

Next, we introduce the time-varying constraint

$$\rho_s(t) < \alpha_s(t, \mathbf{x}_1), \quad \forall t \geq 0, \quad (8)$$

where $\rho_s : \mathbb{R}_{\geq 0} \rightarrow \mathbb{R}_{\leq 0}$ is a continuously differentiable function that remains non-positive. Note that (8) is feasible at all times due to Assumption 7 and since $\rho_s(t) \leq 0$ for all $t \geq 0$. Define

$$\tilde{\Omega}_s(t) := \{\mathbf{x}_1 \in \mathbb{R}^n \mid \alpha_s(t, \mathbf{x}_1) - \rho_s(t) > 0\}, \quad (9)$$

which is the nonempty set where (8) holds. Since $\alpha_s(t, \mathbf{x}_1)$ has compact level curves (i.e., $-\alpha_s(t, \mathbf{x}_1)$ is radially unbounded in \mathbf{x}_1) and $\rho_s(t) \leq 0$, we have $\Omega_s(t) \subseteq \tilde{\Omega}_s(t)$ for all $t \geq 0$; that is, $\tilde{\Omega}_s(t)$ always contains $\Omega_s(t)$. We refer to $\tilde{\Omega}_s(t)$ as the *virtual soft constrained set*.

In this work, we propose a low-complexity control design to ensure (7) and (8) simultaneously along the closed-loop trajectories of (1). In particular, when $\rho_s(t) = 0$ in (8) we have $\Omega_s(t) = \tilde{\Omega}_s(t)$, so enforcing (8) ensures the soft constraints. However, since soft and hard constraints may become incompatible over some time intervals, enforcing both $0 < \alpha_h(t, \mathbf{x}_1)$ and $0 < \alpha_s(t, \mathbf{x}_1)$ might not be feasible for all $t \geq 0$. Thus, $\rho_s(t)$ must be designed so that (7) and (8) can be simultaneously satisfied. Therefore, besides the controller design, a key aspect is to design $\rho_s(t)$ such that $\tilde{\Omega}_s(t)$ remains compatible with the hard constrained set $\Omega_h(t)$ (i.e., $\Omega_h(t) \cap \tilde{\Omega}_s(t) \neq \emptyset$) at all times. For this $\rho_s(t) \leq 0$ should sufficiently decrease whenever the soft and hard constraints are incompatible and it should return back to zero whenever $\Omega_s(t)$ is compatible with $\Omega_h(t)$. To this end, we define $\rho_s(t)$ as

$$\rho_s(t) := \rho_s^n(t) - \rho_s^r(t), \quad (10)$$

where $\rho_s^n : \mathbb{R}_{\geq 0} \rightarrow \mathbb{R}_{\leq 0}$ is a non-positive, continuously differentiable function that serves as the nominal lower bound in (8) to enforce soft constraint satisfaction. The term $\rho_s^r : \mathbb{R}_{\geq 0} \rightarrow \mathbb{R}_{\geq 0}$ is a continuously differentiable non-negative relaxation signal, initialized as $\rho_s^r(0) = 0$, and increases as necessary to ensure compatibility between (7) and (8). In particular, ρ_s^r grows only when enforcing the soft constraints (i.e., $\alpha_s(t, \mathbf{x}_1) > 0$) conflicts with enforcing the hard constraints (i.e., $\alpha_h(t, \mathbf{x}_1) > 0$).

We design $\rho_s^n(t)$ assuming $\rho_s^r(t)$ remains zero (i.e., when hard and soft constraints are always compatible), so that $\rho_s^n(t) = \rho_s(t)$. Specifically, $\rho_s^n(t)$ is chosen to ensure soft constraints are met (at least) within a user-defined finite time T by enforcing (8) on (1), when $\rho_s^r(t) = 0$ for all $t \geq 0$. To this end, $\rho_s^n(t)$ should satisfy:

- (i) If $\alpha_s(0, \mathbf{x}_1(0)) > 0$ (i.e., soft constraints are initially met), then $\rho_s^n(t) = 0$ for all $t \geq 0$.
- (ii) If $\alpha_s(0, \mathbf{x}_1(0)) \leq 0$ (i.e., soft constraints are initially violated), then $\rho_s^n(0) < \alpha_s(0, \mathbf{x}_1(0))$ and $\rho_s^n(t)$ should increase and converge to zero by T seconds (i.e., $\rho_s^n(t \geq T) = 0$).

One possible choice for $\rho_s^n(t)$ is

$$\rho_s^n(t) = \begin{cases} \left(\frac{T-t}{T}\right)^{\frac{1}{1-\beta}} \rho_0, & 0 \leq t \leq T, \\ 0, & t > T, \end{cases} \quad (11)$$

where $\beta \in (0, 1)$ and $\rho_0 := \rho_s^n(0) = \rho_s(0) \leq 0$ are tunable constants.

The design of $\rho_s^r(t)$ is presented in the next subsection.

3.3. Low-Complexity Controller Design

In this subsection, we design a low-complexity robust state feedback controller for (1) that guarantees (7) and (8) at all times. Exploiting the lower triangular structure of (1), we adopt a backstepping-like approach inspired by [10, 32]. For brevity, in the sequel some function arguments are dropped when no ambiguity arises. The controller design steps are summarized as follows:

Step 1-a. Given $\mathbf{x}_1(0)$, compute $\alpha_s(0, \mathbf{x}_1(0))$ and select ρ_0 in (11) such that $\rho_s^n(0) = \rho_s(0) < \alpha_s(0, \mathbf{x}_1(0))$, as detailed in Section 3.2.

Step 1-b. Define

$$e_s(t, \mathbf{x}_1) := \alpha_s(t, \mathbf{x}_1) - \rho_s(t), \quad (12)$$

so that $e_s(t, \mathbf{x}_1) > 0$ for all $t \geq 0$ is equivalent to (8). Next, consider the following (time-varying) reciprocal barrier functions:

$$\varepsilon_h(t, \mathbf{x}_1) := \frac{1}{\alpha_h(t, \mathbf{x}_1)}, \quad (13)$$

$$\varepsilon_s(t, \mathbf{x}_1) := \frac{1}{e_s(t, \mathbf{x}_1)}, \quad (14)$$

Note that establishing the boundedness of ε_h and ε_s for all time ensures that $\alpha_h(t, \mathbf{x}_1)$ and $e_s(t, \mathbf{x}_1)$ remain positive, and thereby guaranteeing the forward invariance of sets $\Omega_h(t)$ in (6a) and $\tilde{\Omega}_s(t)$ in (9), respectively [4].

Step 1-c. Define

$$\mathbf{u}_h := k_h \varepsilon_h^2 \nabla_{\mathbf{x}_1} \alpha_h, \quad (15)$$

where $k_h > 0$. Let $\gamma(t, \mathbf{x}_1) := \varepsilon_h \nabla_{\mathbf{x}_1} \alpha_s^\top \mathbf{G}_1 \nabla_{\mathbf{x}_1} \alpha_h$. We design the following dynamic to govern the evolution of $\rho_s^r(t)$ in (10):

$$\begin{cases} \dot{\rho}_s^r = \phi_\rho(t, \mathbf{x}_1, \rho_s^r) := -\varphi_\gamma \varphi_h \nabla_{\mathbf{x}_1} \alpha_s^\top \mathbf{G}_1 \mathbf{u}_h - k_r \rho_s^r, \\ \rho_s^r(0) = 0, \end{cases} \quad (16)$$

where $k_r > 0$, and $\varphi_h := \varphi(\alpha_h, \delta_h, 0)$ and $\varphi_\gamma := \varphi(\gamma, 0, -\delta_\gamma)$ are \mathcal{C}^1 switch functions, refer to Appendix A for the definition of $\varphi(\cdot, \cdot, \cdot)$, and $\delta_h, \delta_\gamma > 0$ are some sufficiently small tunable constants.

Next, define

$$\mathbf{u}_s := k_s \varepsilon_s^2 \nabla_{\mathbf{x}_1} \alpha_s, \quad (17)$$

where $k_s > 0$. We note that \mathbf{u}_h and \mathbf{u}_s are scaled negative gradients of the reciprocal barrier functions ε_h and ε_s with respect to \mathbf{x}_1 , respectively. The explicit gradient formula of α_h and α_s functions are provided in Appendix B.

Finally, the first intermediate (virtual) control law is designed as

$$\mathbf{s}_1(t, \mathbf{x}_1) := \mathbf{u}_s + \varphi_h \mathbf{u}_h. \quad (18)$$

Step i-a (2 ≤ i ≤ r). Define the i -th intermediate error vector as

$$\mathbf{e}_i = \text{col}(e_{i,j}) := \mathbf{x}_i - \mathbf{s}_{i-1}(t, \bar{\mathbf{x}}_{i-1}), \quad (19)$$

where $\mathbf{e}_i \in \mathbb{R}^n$. Now the goal is to design the i -th intermediate (virtual) control law $\mathbf{s}_i(t, \mathbf{e}_i)$ for (1) to compensate $e_{i,j}(t, \bar{\mathbf{x}}_i)$, $j \in \mathbb{I}_1^n$, by enforcing the following narrowing intermediate constraints

$$-\vartheta_{i,j}(t) < e_{i,j}(t, \bar{\mathbf{x}}_i) < \vartheta_{i,j}(t), \quad j \in \mathbb{I}_1^n, \quad (20)$$

for all $t \geq 0$, where $\vartheta_{i,j} : \mathbb{R}_{\geq 0} \rightarrow \mathbb{R}_{>0}$ are continuously differentiable *strictly positive performance functions* decaying to a neighborhood of zero. One option for $\vartheta_{i,j}(t)$ is:

$$\vartheta_{i,j}(t) := (\vartheta_{i,j}^0 - \vartheta_{i,j}^\infty) \exp(-l_{i,j}t) + \vartheta_{i,j}^\infty, \quad (21)$$

where $l_{i,j}, \vartheta_{i,j}^\infty, \vartheta_{i,j}^0$ are user-defined positive constants. To ensure $e_{i,j}(0, \bar{\mathbf{x}}_i(0)) \in (-\vartheta_{i,j}(0), \vartheta_{i,j}(0))$, select $\vartheta_{i,j}^0 > |e_{i,j}(0, \bar{\mathbf{x}}_i(0))|$.

Step i-b (2 ≤ i ≤ r). Define the diagonal matrix $\Theta_i(t) := \text{diag}(\vartheta_{i,j}(t)) \in \mathbb{R}^{n \times n}$ and consider:

$$\hat{\mathbf{e}}_i(t, \mathbf{e}_i) = \text{col}(\hat{e}_{i,j}) := \Theta_i^{-1}(t) \mathbf{e}_i, \quad (22)$$

as the vector of normalized errors, with elements:

$$\hat{e}_{i,j}(t, e_{i,j}) = \frac{e_{i,j}}{\vartheta_{i,j}(t)}, \quad j \in \mathbb{I}_1^n. \quad (23)$$

Note that $\hat{e}_{i,j} \in (-1, 1)$ iff $e_{i,j} \in (-\vartheta_{i,j}(t), \vartheta_{i,j}(t))$. Next, introduce the following nonlinear transformations

$$\varepsilon_{i,j}(t, \mathbf{e}_i) = \mathcal{T}(\hat{e}_{i,j}) := \ln \left(\frac{1 + \hat{e}_{i,j}}{1 - \hat{e}_{i,j}} \right), \quad j \in \mathbb{I}_1^n, \quad (24)$$

where $\varepsilon_{i,j}$ is the unconstrained transformed signal of $e_{i,j}(t, \bar{\mathbf{x}}_i)$, and $\mathcal{T} : (-1, 1) \rightarrow (-\infty, +\infty)$ is a smooth, strictly increasing bijective mapping with $\mathcal{T}(0) = 0$. Enforcing the boundedness of $\varepsilon_{i,j}$ ensures $\hat{e}_{i,j}$ remains in $(-1, 1)$, thus satisfying (20).

Step i-c (2 ≤ i ≤ r). Design the i -th intermediate control as

$$\mathbf{s}_i(t, \mathbf{e}_i) := -k_i \mathbf{\Xi}_i \mathbf{\varepsilon}_i, \quad (25)$$

where $k_i > 0$ is a control gain, $\mathbf{\varepsilon}_i := \text{col}(\varepsilon_{i,j}) \in \mathbb{R}^n$, and $\mathbf{\Xi}_i := \text{diag}(\xi_{i,j}) \in \mathbb{R}^{n \times n}$ is a diagonal matrix with entries

$$\xi_{i,j}(t, e_{i,j}) := \frac{2}{\vartheta_{i,j}(t) (1 - \hat{e}_{i,j}^2)}, \quad j \in \mathbb{I}_1^n. \quad (26)$$

Note that $\mathbf{s}_i(t, \mathbf{e}_i)$ depends on t and $\bar{\mathbf{x}}_i$ because \mathbf{e}_i itself depends on $\bar{\mathbf{x}}_i$, as seen in (19). Thus, we can write $\mathbf{s}_i(t, \bar{\mathbf{x}}_i)$.

Step r + 1. The control input $\mathbf{u}(t, \mathbf{x})$ is designed as:

$$\mathbf{u}(t, \mathbf{x}) := \mathbf{s}_r(t, \mathbf{x}). \quad (27)$$

Design Philosophy in Step 1: The design begins with an intermediate (virtual) control signal $\mathbf{s}_1(t, \mathbf{x}_1)$ for

the \mathbf{x}_1 dynamics in (1) to guarantee both (7) and (8) constraints are satisfied. More precisely, \mathbf{u}_s and \mathbf{u}_h in (15) and (17) are constructed to meet (7) and (8), respectively. In particular, we utilize the continuously differentiable switch function φ_h for activating and deactivating the effect of \mathbf{u}_h in $\mathbf{s}_1(t, \mathbf{x}_1)$. Note that φ_h becomes active (i.e., $\varphi_h > 0$) when $\alpha_h(t, \mathbf{x}_1(t; \mathbf{x}(0))) < \delta_h$. Hence, the enforcement of hard constraints through \mathbf{u}_h is only applied when the trajectory $\mathbf{x}_1(t; \mathbf{x}(0))$ approaches the boundary of $\text{cl}(\Omega_h(t))$.

For future reference, let us define the sets

$$\Omega_h^{\text{ir}}(t) := \{\mathbf{x}_1 \in \mathbb{R}^n \mid \alpha_h(t, \mathbf{x}_1) \geq \delta_h\}, \quad (28a)$$

$$\Omega_h^{\text{br}}(t) := \{\mathbf{x}_1 \in \mathbb{R}^n \mid 0 < \alpha_h(t, \mathbf{x}_1) < \delta_h\}, \quad (28b)$$

which we call the *interior* and *boundary regions* of the (inner-approximated) time-varying hard-constrained set $\Omega_h(t)$, respectively. Note that $\Omega_h(t) = \Omega_h^{\text{ir}}(t) \cup \Omega_h^{\text{br}}(t)$ and that $\Omega_h^{\text{ir}}(t)$ is nonempty for sufficiently small $\delta_h > 0$ (in particular, when $\alpha_h^*(t) > \delta_h$; see Assumption 7). From (18), when $\mathbf{x}_1(t; \mathbf{x}(0))$ lies in $\Omega_h^{\text{ir}}(t)$, we have $\mathbf{s}_1(t, \mathbf{x}_1) = \mathbf{u}_s$; thus, \mathbf{u}_s remains unaltered to satisfy soft constraints. However, once $\mathbf{x}_1(t; \mathbf{x}(0))$ enters $\Omega_h^{\text{br}}(t)$, the term $\varphi_h \mathbf{u}_h$ begins to influence $\mathbf{s}_1(t, \mathbf{x}_1)$ in (18) to keep the trajectory within $\Omega_h(t)$. Simultaneously, a virtual relaxation of the soft constraints is enacted by expanding $\tilde{\Omega}_s(t)$ (defined in (9)) away from $\Omega_s(t)$ through an increase in ρ_s^r as dictated by (16). This virtual relaxation of soft constraints serves two purposes: (i) ensuring that $\tilde{\Omega}_s(t)$ remains compatible with $\Omega_h(t)$ (i.e., $\Omega_h(t) \cap \tilde{\Omega}_s(t) \neq \emptyset$), and (ii) balancing $\varphi_h \mathbf{u}_h$ with \mathbf{u}_s in (18), thereby confining $\mathbf{x}_1(t; \mathbf{x}(0))$ within the set $\Omega_h(t) \cap \tilde{\Omega}_s(t)$.

Specifically, the first term on the right-hand side (RHS) of (16) is designed to increase $\rho_s(t)$ when necessary. This term is active and positive when both $\varphi_\gamma > 0$ (i.e., when $\gamma = \varepsilon_h \nabla_{\mathbf{x}_1} \alpha_s^\top \mathbf{G}_1 \nabla_{\mathbf{x}_1} \alpha_h < 0$) and $\varphi_h > 0$, and it grows unbounded as $\varepsilon_h \rightarrow +\infty$ (i.e., as $\alpha_h \rightarrow 0$). Specifically, the relaxation signal $\rho_s^r(t)$ increases only when \mathbf{u}_s and \mathbf{u}_h have partially opposing directions (i.e., $\gamma(t, \mathbf{x}_1) < 0$) while the system trajectory is sufficiently close to the boundary of $\text{cl}(\Omega_h(t))$, that is, when $\mathbf{x}_1(t; \mathbf{x}(0)) \in \Omega_h^{\text{ir}}(t)$. In particular, selecting a smaller δ_h and a larger δ_γ in (16) lets the (partial) system trajectory $\mathbf{x}_1(t; \mathbf{x}(0))$ approach the boundary of $\text{cl}(\Omega_h(t))$ more closely before $\tilde{\Omega}_s(t)$ begins to expand.

The second term on the RHS of (16) acts as a stabilizing component, driving $\rho_s(t)$ back to zero exponentially fast when the first term is inactive (i.e., when hard and soft constrained sets are compatible). Moreover, a larger k_r in (16) accelerates the process of recovery of the soft constrained set, i.e., $\tilde{\Omega}_s(t) \rightarrow \Omega_s(t)$, once the soft and hard constrained sets become compatible again.

Design Philosophy of Step 2 ≤ i ≤ r: Similarly to the backstepping approach, the control design continues by crafting a second intermediate control $\mathbf{s}_2(t, \bar{\mathbf{x}}_2)$ for the \mathbf{x}_2 dynamics in (1) so that \mathbf{x}_2 closely tracks $\mathbf{s}_1(t, \mathbf{x}_1)$. In particular, we design this second intermediate control $\mathbf{s}_2(t, \mathbf{e}_1)$ to ensure that all components of the error $\mathbf{e}_2 = \mathbf{x}_2 - \mathbf{s}_1(t, \mathbf{x}_1)$, denoted as $e_{2,j}$, where $j \in \mathbb{I}_1^n$, become

sufficiently small by satisfying (20). This iterative process continues until we obtain $\mathbf{u}(t, \mathbf{x})$ for (1) at *Step r+1*. Notably, unlike the classical backstepping method, we do not use derivatives of $\mathbf{e}_i, i \in \mathbb{I}_2^r$ or any filtering scheme when designing the intermediate control laws $\mathbf{s}_i(t, \mathbf{e}_i), i \in \mathbb{I}_2^r$ [10]. Moreover, our design of (27) does not rely on prior knowledge of the system's nonlinearities or on bounds for uncertainties, making the proposed control approach low-complexity and tractable.

Remark 2. Note that the proposed constraints in (7) and (8), as well as (20) for the intermediate error signals $e_{i,j}, i \in \mathbb{I}_2^r, j \in \mathbb{I}_1^n$, are satisfied merely by keeping ε_h , ε_s , and $\|\varepsilon_i\|$ bounded, respectively. This is achieved by applying the control input (27) in (1). This key observation will aid the stability analysis of the closed-loop system.

Remark 3. Note that the choice of the nonlinear transformation $\varepsilon_{i,j} = \mathcal{T}(\hat{e}_{i,j})$ in (24) is not limited to the log-type function shown in (24). Indeed, any smooth, strictly increasing bijective mapping $\mathcal{T} : (-1, 1) \rightarrow (-\infty, +\infty)$ may be employed. For example, one may opt for the tan-type transformation $\varepsilon_{i,j} = \tan(\frac{\pi}{2}\hat{e}_{i,j})$. Similarly, other reciprocal barrier functions may replace those in (13) and (14). For instance, the log-type reciprocal barrier function [4]: $-\log(\frac{\star}{1+\star})$, with $\star \in \{e_s, \alpha_h\}$, shares similar properties with the inverse-type reciprocal barrier function used in (13) and (14).

3.4. Stability Analysis

Recall that $\nabla_{\mathbf{x}_1} \alpha_h(t, \mathbf{x}_1)$ in (15) and $\nabla_{\mathbf{x}_1} \alpha_s(t, \mathbf{x}_1)$ in (17) denote the control directions in the first intermediate control law $s_1(t, \mathbf{x}_1)$ for satisfying time-varying hard and soft constraints, respectively. Note that $\mathbf{u}_s = 0$ may occur at undesirable (time-varying) critical points of $\alpha_s(t, \mathbf{x}_1)$ outside the soft-constrained set $\Omega_s(t)$, even when $\Omega_s(t)$ is compatible with $\Omega_h(t)$, potentially rendering $s_1(t, \mathbf{x}_1)$ incapable of ensuring soft constraint satisfaction. This issue is avoided if $\nabla_{\mathbf{x}_1} \alpha_s(t, \mathbf{x}_1) = \mathbf{0}_n$ only holds at points where the soft constraints are already met. To this end, we adopt the following technical assumption from [32].

Assumption 9. For all $t \geq 0$, the function $-\alpha_s(t, \mathbf{x}_1)$ is invex, i.e., all critical points of $\alpha_s(t, \mathbf{x}_1)$ are a (time-varying) global maximizer (see [47, Theorem 2.2]).

We note that [32, Lemma 3] provides sufficient conditions on the structure and composition of time-varying soft constraints to ensure Assumption 9. Moreover, from [32, Remark 8], one can infer that this assumption is only sufficient to prevent $\nabla_{\mathbf{x}_1} \alpha_s(t, \mathbf{x}_1)$ from vanishing outside $\Omega_s(t)$; in practice, scenarios often arise where \mathbf{u}_s in (18) effectively satisfies soft constraints even without Assumption 9. Notice that, a similar requirement is unnecessary for $\nabla_{\mathbf{x}_1} \alpha_h(t, \mathbf{x}_1)$ as the partial system trajectory $\mathbf{x}_1(t; \mathbf{x}(0))$ is always required to remain inside $\Omega_h(t)$.

Observe that the time-varying hard constrained set $\Omega_h(t)$ can, in general, decompose into disconnected components in \mathbb{R}^n as time evolves. Hence, mere overall feasibility

(Assumption 7) does not guarantee continuous satisfaction of the hard constraints whenever any component disappears. For example, suppose $\Omega_h(t) = \Omega_h^1(t) \cup \Omega_h^2(t)$ for $t \geq t'$, where each of Ω_h^1 and Ω_h^2 is connected but they are mutually disjoint. Assume further that, for $t \geq t'' > t'$, the component $\Omega_h^1(t)$ vanishes while $\Omega_h^2(t)$ persists. Although $\Omega_h(t)$ remains feasible for $t \geq t''$, a trajectory confined to Ω_h^1 during $t' \leq t < t''$ cannot remain in $\Omega_h(t)$ for $t > t''$ without violating the hard constraints. To avoid this scenario, we adopt the following assumption.

Assumption 10. The set $\Omega_h(t)$ stays connected $\forall t \geq 0$.

Finally, we impose the following regularity assumption on the boundary of the hard-constrained set that streamlines the forthcoming analysis.

Assumption 11. For all $\mathbf{x}_1 \in \{\mathbf{x}_1 \in \mathbb{R}^n \mid \alpha_h(t, \mathbf{x}_1) = 0\}$ and all $t \geq 0$, it holds that $\nabla_{\mathbf{x}_1} \alpha_h(t, \mathbf{x}_1) \neq 0$.

This assumption precludes any critical points on the boundary of the hard-constrained set at all times. Such a non-degenerate boundary is generic and is typically satisfied by standard combinations of hard constraints. Moreover, Assumption 11 implicitly implies Assumption 10. To preserve the connectivity of the feasible hard-constrained set, the boundary $\alpha_h(t, \mathbf{x}_1) = 0$ must stay free of (i) saddle points that would separate multiple regions with $\alpha_h(t, \mathbf{x}_1) > 0$ and $\alpha_h(t, \mathbf{x}_1) < 0$ when $\mathbf{x}_1 \in \mathbb{R}^n, n \geq 2$, and (ii) both saddle points and local minima when $n = 1$.

The following theorem summarizes our main result.

Theorem 1. Consider the MIMO nonlinear system (1) subject to time-varying hard and soft constraints (2). Let $\rho_s(t)$ in (10) be designed according to Subsection 3.2 (i.e., *Step 1-a*) and (16). Moreover, suppose that constants $\vartheta_{i,j}^0, i \in \mathbb{I}_2^r, j \in \mathbb{I}_1^n$ in (21) are selected such that $\vartheta_{i,j}^0 > |e_{i,j}(0, \bar{x}_i(0))|$ (as explained in *Step i-a* in Subsection 3.3). Under Assumptions 1-11, the feedback control law (27) ensures the boundedness of all closed-loop signals as well as the forward invariance of the set $\Omega_h(t) \cap \tilde{\Omega}_s(t)$ for all time.

Proof. See Appendix C. □

Theorem 1 guarantees that the set $\Omega_h(t) \cap \tilde{\Omega}_s(t)$, with $\Omega_h(t)$ and $\tilde{\Omega}_s(t)$ defined in (6a) and (9), respectively, is forward invariant for all $t \geq 0$. Consequently, the state partition $\mathbf{x}_1(t; \mathbf{x}(0))$ always stays inside the hard-constraint set. Forward invariance of $\Omega_h(t) \cap \tilde{\Omega}_s(t)$, however, does not by itself ensure that the soft constraints are respected whenever $\Omega_h(t) \cap \Omega_s(t) \neq \emptyset$ (i.e., compatibility of hard and soft constraints). The relaxation signal $\rho_s(t)$ in (10) is designed so that, when $\Omega_h(t)$ and $\Omega_s(t)$ are mutually compatible, the virtual soft constrained set $\tilde{\Omega}_s(t)$ converges (back) to the true soft constrained set $\Omega_s(t)$. Yet the convergence $\tilde{\Omega}_s(t) \rightarrow \Omega_s(t)$ can fail in certain deadlock situations. Consider, for example, system dynamics (1) that reduce to a single integrator, i.e., $r = 1$, $\mathbf{f}_1(t, \mathbf{x}_1) = \mathbf{0}_n$, and $\mathbf{G}_1(t, \mathbf{x}_1) = \mathbf{I}_n$, so that $\dot{\mathbf{x}}_1 = \mathbf{u}$ with

$\mathbf{u} = \mathbf{s}_1(t, \mathbf{x}_1)$. Suppose the trajectory $\mathbf{x}_1(t; \mathbf{x}_1(0))$ enters and evolves in the boundary region of the hard-constraint set, $\mathbf{x}_1(t; \mathbf{x}_1(0)) \in \Omega_h^{\text{br}}(t)$. If the terms \mathbf{u}_s and $\varphi_h \mathbf{u}_h$ in (18) cancel, we obtain $\mathbf{s}_1(t, \mathbf{x}_1) = \mathbf{0}_n$, and the state can stall at an undesirable equilibrium. Then $\rho_s^r(t)$, governed by (16), may converge to a constant, which keeps $\tilde{\Omega}_s(t)$ apart from $\Omega_s(t)$ even when $\Omega_h(t)$ and $\Omega_s(t)$ are compatible. Such deadlocks can be avoided by the time-varying nature of hard or soft constrained sets, combined with the internal dynamics in (1), which perturb any boundary equilibrium with $\mathbf{s}_1(t, \mathbf{x}_1) = \mathbf{0}_n$, re-activate the evolution of $\rho_s^r(t)$, and restore the desired convergence $\tilde{\Omega}_s(t) \rightarrow \Omega_s(t)$. Example 3 in Section 4 demonstrates this behavior.

Remark 4. *Assumption 11 was introduced solely to streamline the proof of Theorem 1; it is thus a conservative, sufficient condition for the theorem's validity. Example 4 in the simulation study (Section 4) shows that Theorem 1 can still hold even when this assumption is relaxed.*

Remark 5. *The control architecture in Section 3.3 also enables trajectory tracking under time-varying hard constraints. In (18), \mathbf{u}_s may be replaced by any standard tracking controller that, when $\varphi_h \mathbf{u}_h = 0$, drives \mathbf{x}_1 along the reference trajectory. Since this nominal tracking control law remains bounded, Theorem 1 still applies, making the proposed architecture akin to a safety filter. For example, the minimum-norm CBF-QP method of [4] serves as such a filter but requires system model and online optimization. In contrast, our approach is model-free and optimization-free. Furthermore, it not only ensures safety but also enforces prescribed performance in stabilization or tracking by encoding time-varying soft constraints, a capabilities beyond standard CBF-CLF QP designs [4, 14].*

Remark 6. *For brevity, this article focused on time-varying hard and soft constraint sets defined in (6). Each set arises solely from intersecting the corresponding hard or soft constraint functions in (2), implemented via the min operator in (4). In practice, specifications are often more intricate: they may require not only intersections but also unions, or even nested combinations, using both min (for intersections) and max (for unions) across different functions [48]. For time-invariant constraints, [49] proposes a method for constructing a single smooth constraint function whose positive level sets capture such general combinations. Building on this idea, the robust feedback-control strategy developed in this paper may be extendable to handle a broader class of constraints. A detailed investigation of this possibility is left to future work.*

3.5. From Semi-Global to Global Stability Results

We note that the stability results established in Theorem 1 are only semi-global. This is because selecting $\rho_0 = \rho_s(0) < \alpha_s(0, \mathbf{x}_1(0))$ in (11) and $\vartheta_{i,j}^0 > |e_{i,j}(0, \bar{\mathbf{x}}_i(0))|$ in (21) requires knowledge of the system's initial condition $\mathbf{x}(0)$. In addition to tuning these parameters, $\mathbf{x}(0)$ must also be known to implement the proposed state-feedback

control law in (27). In practice, $\mathbf{x}(0)$ is available at the initial time, so one can automatically tune the above parameters before applying the control signal. Nevertheless, certain applications benefit from eliminating parameter tuning at the initial time.

In this section, inspired by [26, 25], we make minor modifications to the control design presented in Section 3.3. This changes eliminates the control scheme's reliance on the system's initial condition, thereby extending the stability guarantees of Theorem 1 from semi-global to global.

Define the *shifting function*

$$\eta(t) = \begin{cases} \varpi(t), & 0 \leq t \leq T_s, \\ 1, & t > T_s, \end{cases} \quad (29)$$

where $\varpi(t)$ is any strictly increasing, continuously differentiable function satisfying $\varpi(0) = 0$ and $\varpi(T_s) = 1$ and $T_s > 0$ is a prescribed settling time. Numerous designs for $\varpi(t)$ are possible; a convenient example is $\varpi(t) = \sin(\frac{\pi}{2} \frac{t}{T_s})$. One can verify that the shifting function $\eta(t)$ is continuously differentiable and that both $\eta(t)$ and its derivative $\dot{\eta}(t)$ remain bounded for all time.

Modified Control Design Scheme: First, we set ρ_0 in (11) to an arbitrary negative constant and ignore whether $\alpha_s(0, \mathbf{x}_1(0)) > 0$ (condition (i) above (11)) holds. Then using the shifting function $\eta(t)$ we redefine e_s in (12) as

$$e_s(t, \mathbf{x}_1) := \eta(t)\alpha_s(t, \mathbf{x}_1) - \rho_s(t). \quad (30)$$

Because $\eta(0) = 0$ and $\rho_0 = \rho_s(0) < 0$, we have $e_s(0, \mathbf{x}_1(0)) > 0$, ensuring that ε_s in (14) is well defined and positive at $t = 0$. Note that, for $t \geq T_s$, (30) reduces to $e_s(t, \mathbf{x}_1) = \alpha_s(t, \mathbf{x}_1) - \rho_s(t)$, which matches the original definition in (12). Unlike Section 3.3, maintaining the boundedness of ε_s in (14) and thus keeping $e_s(t, \mathbf{x}_1)$ in (30), strictly positive guarantees the satisfaction of (8) only for $t \geq T_s$. Moreover, the settling time T_s must satisfy $T_s \leq T$, ensuring that enforcing $e_s(t, \mathbf{x}_1) > 0$ in (30) can ideally satisfy the soft constraints within the user-specified nominal time T .

The modification of e_s in (30) eliminates the need to tune ρ_0 using $\alpha_s(0, \mathbf{x}_1(0))$. Consequently, by adopting (30) in place of (12), one may omit Step 1-a in Section 3.3 and proceed directly with Steps 1-b and 1-c, leading to the first intermediate control law $\mathbf{s}_1(t, \mathbf{x}_1)$ in (18).

Next, to eliminate the need to tune the parameters $\vartheta_{i,j}^0$ in (21) on the basis of $|e_{i,j}(0, \bar{\mathbf{x}}_i(0))|$, we modify the intermediate constraints (20) to

$$-\vartheta_{i,j}(t) < \eta(t)e_{i,j}(t, \bar{\mathbf{x}}_i) < \vartheta_{i,j}(t), \quad j \in \mathbb{I}_1^n, \quad (31)$$

and redefine the normalized error vector $\hat{\mathbf{e}}_i$ in (22) and its components in (23) as $\hat{\mathbf{e}}_i(t, \mathbf{e}_i) = \text{col}(\hat{e}_{i,j}) := \eta(t)\Theta_i^{-1}(t)\mathbf{e}_i$ and

$$\hat{e}_{i,j}(t, e_{i,j}) = \eta(t) \frac{e_{i,j}}{\vartheta_{i,j}(t)}, \quad j \in \mathbb{I}_1^n, \quad (32)$$

respectively. Because $\eta(0) = 0$, the modified intermediate constraints (31) hold automatically at $t = 0$, even

if the original constraints (20) are violated. Specifically, $\hat{e}_{i,j}(0, e_{i,j}(0, \bar{\mathbf{x}}_i(0))) = 0$ for any initial $e_{i,j}(0, \bar{\mathbf{x}}_i(0))$, ensuring that the transformed signals $\varepsilon_{i,j}$ in (24) are equal to zero at the initial time. For $t \geq T_s$, (31) coincides with the original intermediate constraints in (20).

With any positive choice of $\vartheta_{i,j}^0$ and the replacements (31)–(32), one proceeds directly with *Steps i-a* and *i-c* ($2 \leq i \leq r$) in Section 3.3. These steps yield the i -th intermediate control signal $s_i(t, \mathbf{e}_i)$ in (18), whose associated diagonal matrix $\mathbf{\Xi}_i$ has entries

$$\xi_{i,j}(t, e_{i,j}) := \frac{2\eta(t)}{\vartheta_{i,j}(t), (1 - \hat{e}_{i,j}^2)}, \quad j \in \mathbb{I}_1^n. \quad (33)$$

Finally, the control input follows from *Step r+1* as in (27).

The shifting function η is introduced to guarantee that (8) and (20) hold at $t = 0$ for any initial state, without parameter tuning. Consequently, ε_s in (14) and $\varepsilon_{i,j}$ in (24) are initially bounded and well defined. If these quantities remain bounded for all $t \geq 0$, then (8) and (20) are satisfied for all $t \geq T_s$. Thus, the shifting function removes any dependence of the controller parameters on the initial condition, at the cost of postponing the guaranteed satisfaction of the original requirements in (8) and (20) until the finite settling time T_s .

With the above modifications to the control law, we obtain the following corollary, which provides a global stability result that complements Theorem 1.

Corollary 1. *Consider the MIMO nonlinear system (1) subject to the time-varying hard and soft constraints (2). Design $\rho_s(t)$ in (10) as described in Subsection 3.2 and (16), and choose ρ_0 in (11) to be any negative constant. Furthermore, select arbitrary positive constants $\vartheta_{i,j}^0$, $i \in \mathbb{I}_2$, $j \in \mathbb{I}_1^n$, in (21) and for the shifting function in (29), pick $T_s \leq T$. Under Assumptions 1–11, the feedback control law obtained via the modified design scheme of Section 3.5 guarantees that all closed-loop signals remain bounded for all $t \geq 0$ and renders $\Omega_h(t)$ forward invariant for all $t \geq 0$. Moreover, it ensures the forward invariance of the time-varying set $\Omega_h(t) \cap \tilde{\Omega}_s(t)$ for all $t \geq T_s$.*

Proof. The proof follows the same steps as the proof of Theorem 1 in Appendix C and is therefore omitted for brevity. The proof arguments additionally rely on the continuous differentiability of the shifting function $\eta(t)$, together with the boundedness of $\eta(t)$ and $\dot{\eta}(t)$, and on the fact that $\dot{\eta}(t) > 0$ for all $0 \leq t < T$. \square

Remark 7. *Recall that Corollary 1 strengthens the stability result of Theorem 1 from semi-global to global. However, it guarantees the forward invariance of $\Omega_h(t) \cap \tilde{\Omega}_s(t)$ only for all $t \geq T_s$, unlike Theorem 1. This difference stems from the use of the shifting function $\eta(t)$ in (30), whose settling time is T_s . Under the modified control scheme, the boundedness of ε_s established in Corollary 1 implies the forward invariance of $\tilde{\Omega}_s(t)$ for all $t \geq T_s$, while the boundedness of ε_h ensures the forward invariance of the time-varying hard-constrained set $\Omega_h(t)$ for all $t \geq 0$.*

Eq. No.	Parameter(s)
(5)	$\nu = 10$
(11)	$T = 4$, $\beta = 0.3$, $\rho_0 < \alpha(0, \mathbf{x}_1(0))$
(15)	$k_h = 1$
(16)	$\delta_h = 0.5$, $\delta_\gamma = 10$, $k_r = 1.5$
(17)	$k_s = 1$
(21)	$\vartheta_{2,j}^\infty = 0.1$, $l_{2,j} = 1$, $\vartheta_{2,j}^0 > e_{2,j}(0, \bar{\mathbf{x}}_2(0)) $, $j \in \mathbb{I}_1^2$
(25)	$k_2 = 1$

Table 1: Control-law parameters.

4. Simulation Results

This section presents several simulation examples to validate the proposed approach. We consider the position control problem of a unicycle mobile robot on a 2D plane subject to soft and hard spatiotemporal specifications.¹

The uncertain mobile robot dynamics are given by

$$\begin{cases} \dot{\mathbf{p}}_c = \mathbf{S}(\theta)\zeta \\ \bar{\mathbf{M}}\dot{\zeta} + \bar{\mathbf{D}}\zeta = \bar{\mathbf{u}} + \bar{\mathbf{d}}(t) \end{cases}, \quad \mathbf{S}(\theta) = \begin{bmatrix} \cos \theta & \sin \theta & 0 \\ 0 & 0 & 1 \end{bmatrix}^\top. \quad (34)$$

where $\mathbf{p}_c = [x_c, y_c, \theta]^\top$ denotes the robot position and orientation, and $\zeta = [v_T, \dot{\theta}]^\top$ denotes the translational speed v_T along θ and the angular speed $\dot{\theta}$ about the vertical axis through the robot's center of mass. In (34), $\bar{\mathbf{D}} = \text{diag}(\bar{D}_1, \bar{D}_2)$ is an unknown constant damping matrix, and $\bar{\mathbf{M}} = \text{diag}(m_R, I_R)$ with $m_R > 0$, $I_R > 0$ the unknown mass and moment of inertia about the vertical axis. The input $\bar{\mathbf{u}}$ is the force/torque vector, and $\bar{\mathbf{d}}(t)$ collects bounded external disturbances.

Selecting a virtual control point (VCP) on the robot transforms the underactuated dynamics in (34) into a fully actuated system; see [50]. We therefore apply the VCP transformation to obtain

$$\begin{aligned} \dot{\mathbf{x}}_1 &= \mathbf{x}_2, \\ \dot{\mathbf{x}}_2 &= \mathbf{M}(\mathbf{x}_1)^{-1}(-\mathbf{C}(\mathbf{x}_1, \mathbf{x}_2)\mathbf{x}_2 - \mathbf{D}(\mathbf{x}_1)\mathbf{x}_2 + \mathbf{u} + \mathbf{d}(t)), \end{aligned} \quad (35)$$

where $\mathbf{x}_1 = [x_{1,1}, x_{1,2}]^\top := [x_c, y_c]^\top + L[\cos \theta, \sin \theta]^\top$ is the VCP located L units ahead of the center of mass along the heading, and \mathbf{x}_2 is its velocity. Details of the transformation matrix and the correspondence between the models in (35) and (34) can be found in [32, 50]. The mappings $\mathbf{M}(\mathbf{x}_1)$, $\mathbf{C}(\mathbf{x}_1, \mathbf{x}_2)$, and $\mathbf{D}(\mathbf{x}_1)$ are locally Lipschitz, with \mathbf{M} positive definite. Note that (35) is a particular form of (1) with $n = 2$ and $r = 2$, satisfying Assumptions 1–3. In the simulations we set $m_R = 3.6$, $I_R = 0.0405$, $\bar{D}_1 = 0.3$, $\bar{D}_2 = 0.04$, $L = 0.2$, and $\bar{\mathbf{d}}(t) = [0.75 \sin(3t + \frac{\pi}{3}) + 1.5 \cos(t + \frac{3\pi}{7}), -0.8 \exp(\cos(t + \frac{\pi}{3}) + 1) \sin(t)]^\top$.

Example 1: Assume that the ground robot should stay within a circular zone directly beneath an aerial survey robot while operating in a confined workspace. We model the workspace with the (time-invariant) \mathcal{C}^1 hard

¹Simulations video: https://youtu.be/EAbVfd9_BLE

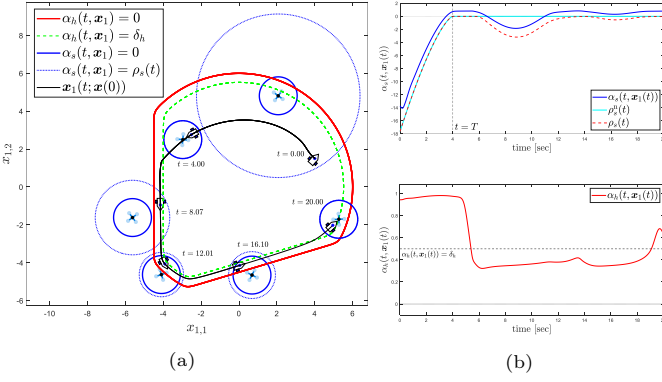


Figure 1: Simulation results of Example 1: Initial condition dependent tuning of the control law.

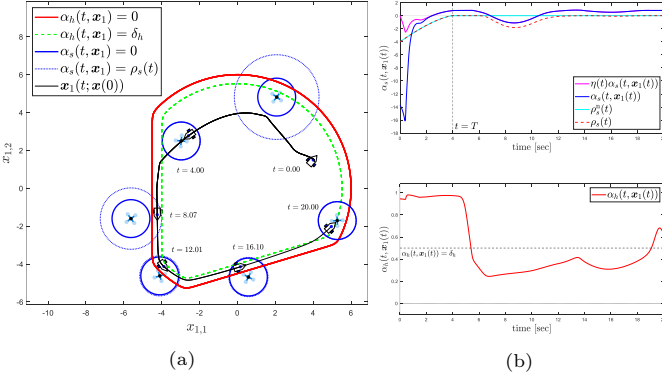


Figure 2: Simulation results of Example 1: Initial condition free control law and a larger δ_γ .

constraints $\psi_{h_1}(\mathbf{x}_1) = x_{1,1} + 4.5 > 0$, $\psi_{h_2}(\mathbf{x}_1) = x_{1,2} - 0.3x_{1,1} + 4.5 > 0$, and $\psi_{h_3}(\mathbf{x}_1) = \tanh(0.1(36 - \|\mathbf{x}_1\|^2)) > 0$.² The task is encoded by the time-varying soft constraint $\psi_s(t, \mathbf{x}_1) = 1 - \|\mathbf{x}_1 - \mathbf{x}_a^p(t)\|^2 > 0$, i.e., a unit-radius disk centered at the ground projection $\mathbf{x}_a^p(t) := [x_{a,1}(t), x_{a,2}(t)]^\top$ of the aerial robot's position.

Table 1 lists the numerical values used to implement the control law (27). The parameters ρ_0 and $\vartheta_{2,j}^0$, $j \in \mathbb{I}_1^2$, are tuned based on the initial state $\mathbf{x}(0)$ of the transformed dynamics (35). Henceforth, for brevity we write $\mathbf{x}_1(t)$ instead of $\mathbf{x}_1(t; \mathbf{x}(0))$.

Fig.1a shows snapshots of the robot's VCP trajectory under the proposed controller. The VCP remains inside the workspace, whose boundary $\alpha_h = 0$ (solid red) encloses the hard-constraint set Ω_h , while the robot strives to enter and stay within the 1m horizontal radius of the aerial robot, whose boundary $\alpha_s = 0$ (solid blue) encloses the (time-varying) soft-constraint set $\Omega_s(t)$. Fig.1b depicts the evolution of the consolidated soft constraint $\alpha_s(t; \mathbf{x}_1(t))$ (top) and hard constraint $\alpha_h(t; \mathbf{x}_1(t))$ (bottom) functions along the robot's VCP trajectory.

As shown in Fig.1a, when the robot enters the boundary region of the hard constrained set Ω_h^{br} with $0 < \alpha_h < \delta_h$ (green dashed curve), the term \mathbf{u}_h in (18) switches on and

keeps the robot inside the safe region. If the nominal soft set tries to leave the hard set, active deviation of $\rho_s(t)$ from its nominal value $\rho_s^0(t)$ (Fig.1b, top) enlarges the virtual soft set $\tilde{\Omega}_s(t)$ in (9) (dotted blue curve in Fig.1a) just enough to keep it compatible with the hard constraints. Figs.1a and 1b (top) confirm that the (compatible) soft constraint is met within the user-defined time $T = 4$. Fig.1b (bottom) shows that the hard constraint is never violated, as $\alpha_h(t; \mathbf{x}_1(t))$ stays strictly positive under the proposed controller.

To illustrate the effect of tuning δ_γ parameter of φ_γ in (16) and the initial-condition-free control law of Section 3.5, we re-conducted the simulation; the results appear in Fig.2. The choice of parameters match Table 1 except for arbitrary selection of $\rho_0 = -4$, $\vartheta_{2,1} = \vartheta_{2,2} = 1$, and setting the shifting function's settling time to $T_s = T = 4$. Moreover, we set $\delta_\gamma = 40$.

Fig.2a shows the robot initially outside $\tilde{\Omega}_s(0)$ (dashed blue circle). In particular usage of the shifting function $\eta(t)$ keeps the modified controller well-posed and restores the desired behavior for $t > T_s = 4$. Fig.2b (top) depicts the evolution of $\eta(t)\alpha_s(t, \mathbf{x}_1(t))$ which was used in (30); it is a scaled version of $\alpha_s(t, \mathbf{x}_1(t))$ for $0 \leq t \leq T_s$ and equals $\alpha_s(t, \mathbf{x}_1(t))$ once $\eta(t) = 1$. Clearly, the proposed modified control scheme keeps $\eta(t)\alpha_s(t, \mathbf{x}_1(t)) - \rho_s(t) > 0$, $\forall t > 0$.

As mentioned in Section 3.3 a larger δ_γ yields a less conservative expansion of the virtual soft set when the VCP approaches the hard set's boundary, as seen by comparing snapshots at $t = 8.07$, 12.01 , and 16.10 in Figs.1a and 2a. Therefore, the soft constraint is violated for a shorter interval that is roughly $t \in [7, 10.5]$ in Fig.2b (top) versus $t \in [6.5, 11.5]$ in Fig.1b (top).

Example 2: Here, we study a scenario similar to Example 1, in which a time-varying hard constrained set bounds the ground robot's workspace and accounts for moving obstacles. We also impose soft constraints requiring the ground robot to stay within a rectangular region beneath the aerial robot. In particular, the soft constraints are defined as $\psi_{s_1}(t, \mathbf{x}_1) = 1 - (x_{1,1} - x_{a,1}(t)) > 0$, $\psi_{s_2}(t, \mathbf{x}_1) = (x_{1,1} - x_{a,1}(t)) + 1 > 0$, $\psi_{s_3}(t, \mathbf{x}_1) = 1 - (x_{1,2} - x_{a,2}(t)) > 0$, $\psi_{s_4}(t, \mathbf{x}_1) = (x_{1,2} - x_{a,2}(t)) + 1 > 0$. The hard constraints are $\psi_{h_1}(\mathbf{x}_1) = 7 - x_{1,1} > 0$, $\psi_{h_2}(\mathbf{x}_1) = x_{1,1} + 7 > 0$, $\psi_{h_3}(\mathbf{x}_1) = 4 - x_{1,2} > 0$, $\psi_{h_4}(\mathbf{x}_1) = x_{1,2} + 4 > 0$, $\psi_{h_5}(t, \mathbf{x}_1) = \tanh(0.7(r_1^2 - |\mathbf{x}_1 - \mathbf{x}_{c_1}(t)|^2)) > 0$, $\psi_{h_6}(t, \mathbf{x}_1) = \tanh(0.7(r_2(t)^2 - |\mathbf{x}_1 - \mathbf{x}_{c_2}(t)|^2)) > 0$, $\psi_{h_7}(t, \mathbf{x}_1) = (\mathbf{x}_1 - \mathbf{x}_e(t))^\top \mathbf{A}(t) (\mathbf{x}_1 - \mathbf{x}_e(t)) - 1 > 0$, where $\psi_{h_1}, \dots, \psi_{h_4}$ define the workspace boundary, ψ_{h_5} and ψ_{h_6} correspond to moving circular obstacles, and ψ_{h_7} represents a moving and rotating elliptical obstacle. In simulation we choose $r_1 = 1.2$ and $r_2(t) = 1.2 + 0.3 \sin(0.5t)$ for the obstacle radii, with centers $\mathbf{x}_{c_1}(t) = [0, -1.7 \cos(0.3t)]^\top$, $\mathbf{x}_{c_2}(t) = [-4, -1.3 \sin(0.15t)]^\top$, and $\mathbf{x}_e(t) = [4, 1.5 \sin(0.3t)]^\top$. The matrix $\mathbf{A}(t) = \mathbf{R}(\theta_e(t)) \text{diag}(a_e, b_e) \mathbf{R}(\theta_e(t))^\top$, where $\mathbf{R}(\theta_e(t)) \in SO(2)$ is a rotation matrix with a time-varying rotation of $\theta_e(t) = 2\pi \cos(0.2t)$, and $a_e = 1.6$, $b_e = 1$.

²The monotone map $\tanh(\cdot)$ is used only for clearer plots; its zero super-level set matches that of $36 - \|\mathbf{x}_1\|^2$. The scaling feature of $\tanh(\cdot)$ can also help with the numerical conditioning [49].

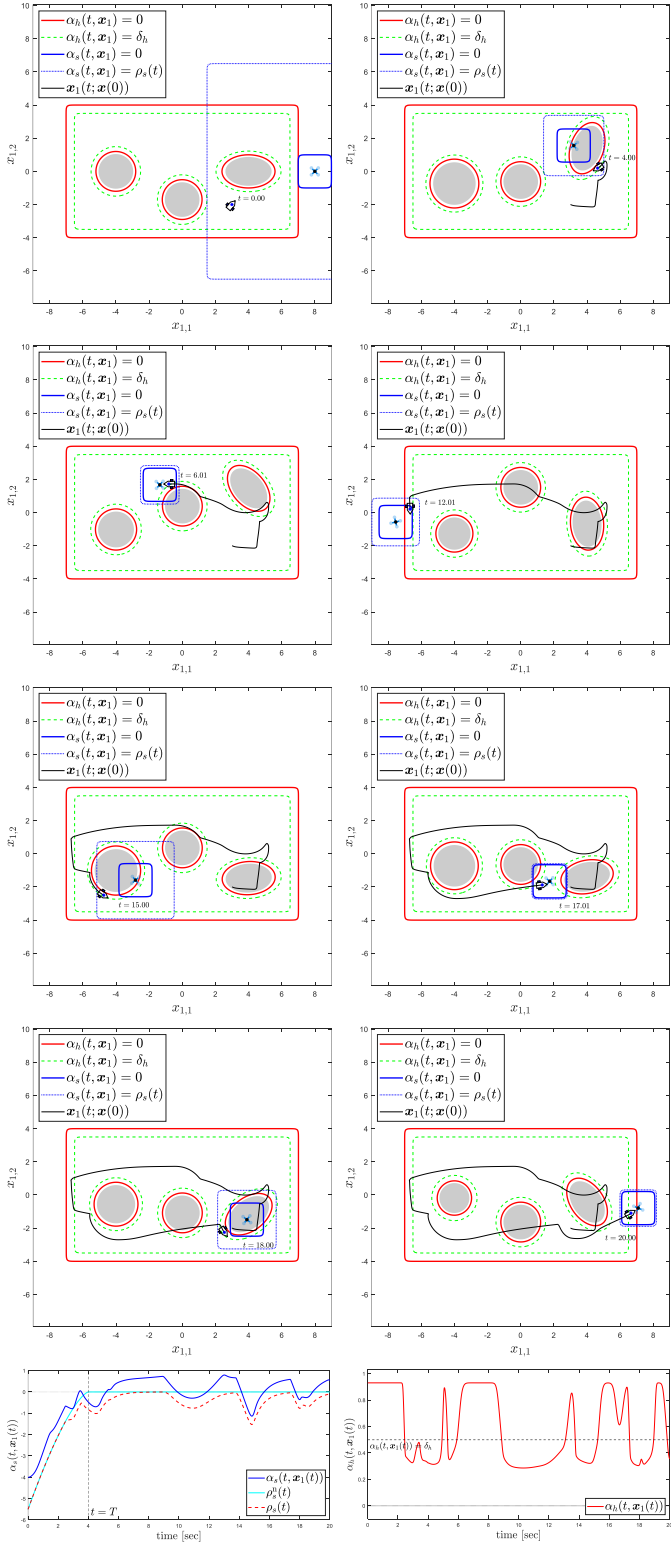


Figure 3: Simulation results of Example 2.

are the ellipse semi-axes. All controller parameters match Table 1. Fig.3 illustrates snapshots of the mobile robot's trajectory along with the evolution of $\alpha_s(t; \mathbf{x}_1(t))$ (bottom left) and $\alpha_h(t; \mathbf{x}_1(t))$ (bottom right).

Example 3: As noted below Theorem 1, the closed-loop system can, under certain conditions, settle at undesired equilibria located on the boundary region of the hard constrained set. In these cases, although Theorem 1 guarantees satisfaction of the hard constraints for all time, it does not necessarily ensure that $\mathbf{x}_1(t)$ will respect the soft constraint, even when the soft and hard constraints are mutually compatible. To illustrate this point, we present a simulation in which the ground robot's VCP is subject to the time-invariant hard constraints $\psi_h(\mathbf{x}_1) = 7 - x_{1,1} > 0$, $\psi_h(\mathbf{x}_1) = x_{1,1} + 7 > 0$, $\psi_h(\mathbf{x}_1) = 4 - x_{1,2} > 0$, $\psi_h(\mathbf{x}_1) = x_{1,2} + 4 > 0$, and $\psi_h(\mathbf{x}_1) = \tanh(0.7(r_1^2 - \|\mathbf{x}_1 - \mathbf{x}_c\|^2)) > 0$ with $r_1 = 1.2$ and $\mathbf{x}_c = [0, 0]^\top$, which model the bounded workspace together with a stationary circular obstacle at the origin. As in Example 1, the soft constraint is defined as $\psi_s(t, \mathbf{x}_1) = 1 - \|\mathbf{x}_1 - \mathbf{x}_a^p(t)\|^2 > 0$.

Consider now the special case in which the external disturbance vector in (34) is zero, the aerial robot remains stationary at $\mathbf{x}_a^p = [4, 0]^\top$, and the ground robot's initial position lies on the line through the obstacle center and \mathbf{x}_a^p . The controller parameters are identical to those in Example 2. Fig.4 shows the resulting trajectories. Despite the compatibility of hard and soft constraints, the ground robot fails to reach its goal and instead converges to an equilibrium on the boundary of the hard constrained set (this is evident from the evolution of $\alpha_h(t, \mathbf{x}_1(t))$). At this equilibrium, the terms \mathbf{u}_s and $\varphi_h \mathbf{u}_h$ cancel in (18). It can be inferred that the domain of attraction of this undesired equilibrium lies to its left, along the line connecting the aerial robot and the obstacle center. Starting from any other initial condition, however, does not drive the ground robot to this equilibrium.

Finally, we emphasize that such undesired equilibria are effectively unstable in practice. More precisely, when even small disturbances are present in the ground robot's dynamics or when the constraints are slightly time-varying such undesired equilibria show an unstable behavior. To demonstrate this, let the aerial robot exhibit small oscillations, $\mathbf{x}_a^p(t) = [4 + 0.01 \sin(t), 0.01 \cos(0.3t)]^\top$, which makes the soft constraint time-varying but with negligible magnitude. Repeating the simulation under this condition yields the results in Fig.5. The ground robot escapes the undesired equilibrium and ultimately completes its task. This example shows that, when undesired equilibria exist, a mild time-varying behavior in the constraints or internal dynamics of the system can mitigate their impact on the closed-loop system behavior.

Example 4: Followed by Remark 4, to clarify that relaxing Assumption 11 may not influence the proposed control law's effectiveness, here, we consider a simulation setup akin to Example 1 with the difference that this time the mobile robot is subjected to the following hard constraint $\psi_h(\mathbf{x}_1) = (4.5 - \|\mathbf{x}_1\|)^3 > 0$. Notice that $\psi_h(\mathbf{x}_1) > 0$ represents a stationary circular region and we also have $\alpha_h(\mathbf{x}_1) = \psi_h(\mathbf{x}_1)$. It is easy to verify that gradient of $\alpha_h(\mathbf{x}_1)$ vanishes all over the boundary of the hard constraint where $\alpha_h(\mathbf{x}_1) = 0$. Indeed, one can verify that the level curve $\alpha_h(\mathbf{x}_1) = 0$ is constituted by a continuum of (degenerate) saddle points. For this simulation

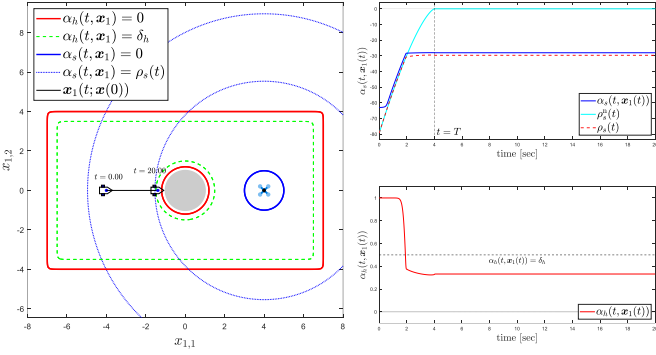


Figure 4: Simulation results for Example 3: existence of an undesired equilibrium in the closed-loop system under stationary constraints.

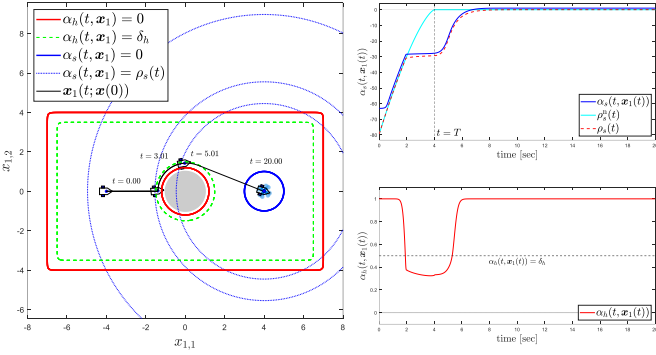


Figure 5: Simulation results for Example 3: escaping the undesired equilibrium under a mildly time-varying soft constraint

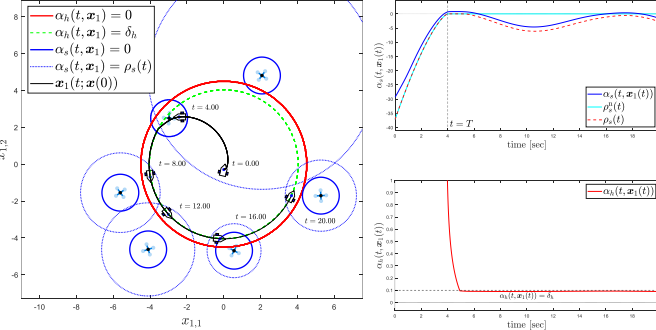


Figure 6: Simulation results of Example 4.

the numerical values of all controller parameters are the same as Example 1 except for $\delta_h = 0.1$. As Fig.6 suggests the proposed control law is still effective even when Assumption 11 does not hold.

5. Conclusions

In this work, we present a robust, closed-form control framework for uncertain, high-relative-degree nonlinear MIMO systems subjected to time-varying hard (safety) and soft (performance) constraints. All constraints are first condensed into scalar hard- and soft-constraint functions whose time-varying zero super-level sets delineate the regions where the corresponding constraints hold. Reciprocal barrier functions are then used for designing ro-

bust explicit velocity-level control laws that enforce both constraint classes. When safety and performance requirements contravene, an innovative dynamic-relaxation scheme temporarily loosens the soft constraints, ensuring that hard constraints are never violated. Finally by carefully chosen nonlinear transformations, followed by a low-complexity backstepping-like design, we extended the velocity-level law to actual control inputs without resorting to approximation schemes for coping with system uncertainties. Furthermore, we showed that by embedding shifting functions into the controller design one can decouple controller-parameter tuning from initial conditions, upgrading the stability guarantees from semi-global to global. In the future, we plan to relax Assumption 11 and extend the results to cooperative control of multi-agent systems.

Appendix A. Definition of \mathcal{C}^1 switch function

The continuously differentiable switching function $\varphi : \mathbb{R} \times \mathbb{R} \times \mathbb{R} \rightarrow [0, 1]$ is defined as

$$\varphi(\chi, \bar{b}, \underline{b}) := \begin{cases} 0 & \chi > \bar{b} \\ a_3\chi^3 + a_2\chi^2 + a_1\chi + a_0 & \underline{b} \leq \chi \leq \bar{b} \\ 1 & \chi < \underline{b} \end{cases} \quad (\text{A.1})$$

where $\bar{b} > \underline{b}$. The coefficients of the cubic polynomial can be obtained via solving the following linear matrix equation for given \bar{b} and \underline{b} , refer to [51, Section 7.5.1] for more information.

$$\begin{bmatrix} 1 & \bar{b} & \bar{b}^2 & \bar{b}^3 \\ 0 & 1 & 2\bar{b} & 3\bar{b}^2 \\ 1 & \underline{b} & \underline{b}^2 & \underline{b}^3 \\ 0 & 1 & 2\underline{b} & 3\underline{b}^2 \end{bmatrix} \begin{bmatrix} a_0 \\ a_1 \\ a_2 \\ a_3 \end{bmatrix} = \begin{bmatrix} 0 \\ 0 \\ 1 \\ 0 \end{bmatrix}. \quad (\text{A.2})$$

In general, solving (A.2) yields:

$$a_0 = \frac{\bar{b}^2(3\underline{b} - \bar{b})}{(\underline{b} - \bar{b})^3}, \quad a_1 = \frac{-6\bar{b}\underline{b}}{(\underline{b} - \bar{b})^3}, \quad a_2 = \frac{3(b + \bar{b})}{(\underline{b} - \bar{b})^3}, \quad a_3 = \frac{-2}{(\underline{b} - \bar{b})^3}.$$

Appendix B. Gradients and partial time derivatives of α_h and α_s

The gradients of functions α_h and α_s in (5) are

$$\begin{aligned} \nabla_{\mathbf{x}_1} \alpha_{\star}(t, \mathbf{x}_1) &= \frac{\sum_{j=1}^{m_{\star}} \frac{\partial \psi_{\star j}(t, \mathbf{x}_1)}{\partial \mathbf{x}_1}^{\top} e^{-\nu \psi_{\star j}(t, \mathbf{x}_1)}}{\sum_{j=1}^{m_{\star}} e^{-\nu \psi_{\star j}(t, \mathbf{x}_1)}} \\ &= \left(\sum_{j=1}^{m_{\star}} \frac{\partial \psi_{\star j}(t, \mathbf{x}_1)}{\partial \mathbf{x}_1}^{\top} e^{-\nu \psi_{\star j}(t, \mathbf{x}_1)} \right) e^{\nu \alpha_{\star}(t, \mathbf{x}_1)}, \end{aligned}$$

where $\star \in \{h, s\}$. Moreover, the partial time derivative of α_h and α_s in (5) are given as the following scalar functions

$$\begin{aligned} \frac{\partial \alpha_{\star}(t, \mathbf{x}_1)}{\partial t} &= \frac{\sum_{j=1}^{m_{\star}} \frac{\partial \psi_{\star j}(t, \mathbf{x}_1)}{\partial t} e^{-\nu \psi_{\star j}(t, \mathbf{x}_1)}}{\sum_{j=1}^{m_{\star}} e^{-\nu \psi_{\star j}(t, \mathbf{x}_1)}} \\ &= \left(\sum_{j=1}^{m_{\star}} \frac{\partial \psi_{\star j}(t, \mathbf{x}_1)}{\partial t} e^{-\nu \psi_{\star j}(t, \mathbf{x}_1)} \right) e^{\nu \alpha_{\star}(t, \mathbf{x}_1)}. \end{aligned}$$

Appendix C. Proof of Theorem 1

From (19) we have $\mathbf{x}_2 = \mathbf{e}_2 + \mathbf{s}_1(t, \mathbf{x}_1)$, $\mathbf{x}_3 = \mathbf{e}_3 + \mathbf{s}_2(t, \mathbf{x}_2)$ and $\mathbf{x}_i = \mathbf{e}_i + \mathbf{s}_{i-1}(t, \mathbf{x}_{i-1})$, $i \in \mathbb{I}_4^r$. As a result, with a slight abuse of notation, from (22) one can recursively write

$$\mathbf{x}_2 = \Theta_2^{-1}(t) \hat{\mathbf{e}}_2 + \mathbf{s}_1(t, \mathbf{x}_1), \quad (\text{C.1a})$$

$$\mathbf{x}_3 = \Theta_3^{-1}(t) \hat{\mathbf{e}}_3 + \mathbf{s}_2(t, \mathbf{x}_1, \hat{\mathbf{e}}_2), \quad (\text{C.1b})$$

$$\mathbf{x}_i = \Theta_i^{-1}(t) \hat{\mathbf{e}}_i + \mathbf{s}_{i-1}(t, \mathbf{x}_1, \hat{\mathbf{e}}_2, \dots, \hat{\mathbf{e}}_{i-1}), \quad i \in \mathbb{I}_4^r. \quad (\text{C.1c})$$

Now from (1) and (C.1a) we have

$$\dot{\mathbf{x}}_1 := \phi_1(t, \mathbf{x}_1, \hat{\mathbf{e}}_2) \quad (\text{C.2})$$

$$= \mathbf{f}_1(t, \mathbf{x}_1) + \mathbf{G}_1(t, \mathbf{x}_1) (\Theta_2^{-1}(t) \hat{\mathbf{e}}_2 + \mathbf{s}_1(t, \mathbf{x}_1)).$$

Taking the time derivative of (5a) leads to

$$\dot{\alpha}_h := \phi_h(t, \mathbf{x}_1, \hat{\mathbf{e}}_2) = \frac{\partial \alpha_h(t, \mathbf{x}_1)}{\partial \mathbf{x}_1} \dot{\mathbf{x}}_1 + \frac{\partial \alpha_h(t, \mathbf{x}_1)}{\partial t}. \quad (\text{C.3})$$

Using (10) and (16), one can obtain the time derivative of (12) as follows

$$\begin{aligned} \dot{\mathbf{e}}_s &:= \phi_s(t, \mathbf{x}_1, \hat{\mathbf{e}}_2, \rho_s^r) \quad (\text{C.4}) \\ &= \frac{\partial \alpha_s(t, \mathbf{x}_1)}{\partial \mathbf{x}_1} \dot{\mathbf{x}}_1 + \frac{\partial \alpha_s(t, \mathbf{x}_1)}{\partial t} - \dot{\rho}_s^r(t) + \phi_\rho(t, \mathbf{x}_1, \rho_s^r). \end{aligned}$$

Moreover, differentiating (22) with respect to time and substituting equations (1), (C.1), and (27) results in:

$$\begin{aligned} \dot{\hat{\mathbf{e}}}_2 &:= \phi_2(t, \mathbf{x}_1, \hat{\mathbf{e}}_2, \hat{\mathbf{e}}_3) \quad (\text{C.5a}) \\ &= \Theta_2^{-1}(t) \left[\mathbf{f}_2(t, \mathbf{x}_1, \hat{\mathbf{e}}_2) + \mathbf{G}_2(t, \mathbf{x}_1, \hat{\mathbf{e}}_2) (\Theta_3^{-1}(t) \hat{\mathbf{e}}_3 \right. \\ &\quad \left. + \mathbf{s}_2(t, \mathbf{x}_1, \hat{\mathbf{e}}_2)) - \dot{\mathbf{s}}_1(t, \mathbf{x}_1) - \dot{\Theta}_2(t) \hat{\mathbf{e}}_2 \right], \end{aligned}$$

$$\begin{aligned} \dot{\hat{\mathbf{e}}}_i &:= \phi_i(t, \mathbf{x}_1, \hat{\mathbf{e}}_2, \dots, \hat{\mathbf{e}}_i) \quad (\text{C.5b}) \\ &= \Theta_i^{-1}(t) \left[\mathbf{f}_i(t, \mathbf{x}_1, \hat{\mathbf{e}}_2, \dots, \hat{\mathbf{e}}_i) + \mathbf{G}_i(t, \mathbf{x}_1, \hat{\mathbf{e}}_2, \dots, \hat{\mathbf{e}}_i) \right. \\ &\quad \times (\Theta_{i+1}^{-1}(t) \hat{\mathbf{e}}_{i+1} + \mathbf{s}_i(t, \mathbf{x}_1, \hat{\mathbf{e}}_2, \dots, \hat{\mathbf{e}}_i)) \\ &\quad \left. - \dot{\mathbf{s}}_{i-1}(t, \mathbf{x}_1, \hat{\mathbf{e}}_2, \dots, \hat{\mathbf{e}}_{i-1}) - \dot{\Theta}_i(t) \hat{\mathbf{e}}_i \right], \quad i \in \mathbb{I}_3^{r-1}, \end{aligned}$$

$$\begin{aligned} \dot{\hat{\mathbf{e}}}_r &:= \phi_r(t, \mathbf{x}_1, \hat{\mathbf{e}}_2, \dots, \hat{\mathbf{e}}_r) \quad (\text{C.5c}) \\ &= \Theta_r^{-1}(t) \left[\mathbf{f}_r(t, \mathbf{x}_1, \hat{\mathbf{e}}_2, \dots, \hat{\mathbf{e}}_r) + \mathbf{G}_r(t, \mathbf{x}_1, \hat{\mathbf{e}}_2, \dots, \hat{\mathbf{e}}_r) \right. \\ &\quad \times \mathbf{u}(t, \mathbf{x}_1, \hat{\mathbf{e}}_2, \dots, \hat{\mathbf{e}}_r) - \dot{\mathbf{s}}_{r-1}(t, \mathbf{x}_1, \hat{\mathbf{e}}_2, \dots, \hat{\mathbf{e}}_{r-1}) \\ &\quad \left. - \dot{\Theta}_r(t) \hat{\mathbf{e}}_r \right], \end{aligned}$$

Now, let us define $\mathbf{z} := [\mathbf{x}_1^\top, \alpha_h, \rho_s^r, \mathbf{e}_s, \hat{\mathbf{e}}_2^\top, \dots, \hat{\mathbf{e}}_r^\top]^\top \in \mathbb{R}^{nr+3}$ and consider the dynamical system

$$\dot{\mathbf{z}} = \phi(t, \mathbf{z}) := \begin{bmatrix} \phi_1(t, \mathbf{x}_1, \hat{\mathbf{e}}_2) \\ \phi_h(t, \mathbf{x}_1, \hat{\mathbf{e}}_2) \\ \phi_\rho(t, \mathbf{x}_1, \rho_s^r) \\ \phi_s(t, \mathbf{x}_1, \hat{\mathbf{e}}_2, \rho_s^r) \\ \phi_2(t, \mathbf{x}_1, \hat{\mathbf{e}}_2, \hat{\mathbf{e}}_3) \\ \vdots \\ \phi_r(t, \mathbf{x}_1, \hat{\mathbf{e}}_2, \dots, \hat{\mathbf{e}}_r) \end{bmatrix}, \quad (\text{C.6})$$

as well as the (nonempty) open set: $\Omega_{\mathbf{z}} := \mathbb{R}^n \times (0, +\infty) \times \mathbb{R} \times (0, +\infty) \times \underbrace{(-1, 1)^n \times \dots \times (-1, 1)^n}_{(r-1) \text{ times}}$.

In what follows, we proceed in three phases. First, we show that a unique, maximal solution $\mathbf{z} : [0, \tau_{\max}) \rightarrow \mathbb{R}^{nr+3}$ for (C.6) exists over $\Omega_{\mathbf{z}}$ (i.e., $\mathbf{z}(t; \mathbf{z}(0)) \in \Omega_{\mathbf{z}}$ for all $t \in [0, \tau_{\max})$). Next, we prove that the control scheme guarantees for all $t \in [0, \tau_{\max})$ that (a) the closed-loop signals in (C.6) are bounded, and (b) $\mathbf{z}(t; \mathbf{z}(0))$ remains strictly within a compact subset of $\Omega_{\mathbf{z}}$, which leads by contradiction to $\tau_{\max} = +\infty$ (i.e., forward completeness) in the final phase. Note that the latter implies α_h , e_s , and $\hat{\mathbf{e}}_i$, $i \in \mathbb{I}_2^r$ remain in strict subsets of $(0, +\infty)$, $(0, +\infty)$, and $(-1, 1)^n$, respectively, thus satisfying (7), (8), and (20).

Phase I: The set $\Omega_{\mathbf{z}}$, defined below (C.6), is nonempty, open, and time-invariant. Moreover, for any initial condition $\mathbf{x}(0)$ in (1), Assumption 8 ensures $\alpha_h(0, \mathbf{x}_1(0)) \in (0, +\infty)$, and by the design of $\rho_s(t)$ in (10) we have $\alpha_s(0, \mathbf{x}_1(0)) > \rho_s(0)$, hence, $e_s(0, \mathbf{x}_1(0)) \in (0, +\infty)$. Additionally, as noted in *Step i-a* of Subsection 3.3, the parameters $\vartheta_{i,j}^0$ in (21) are chosen so that $\vartheta_{i,j}^0 > |e_{i,j}(0, \bar{x}_i(0))|$, ensuring $\hat{e}_{i,j}(0, \bar{x}_i(0)) \in (-1, 1)$ for all $j \in \mathbb{I}_1^n$ and $i \in \mathbb{I}_2^r$. Hence, for all $i \in \mathbb{I}_2^r$ we have $\hat{e}_i(0, \bar{x}_i(0)) \in (-1, 1)^n$. These collectively imply that $\mathbf{z}(0) \in \Omega_{\mathbf{z}}$. Furthermore, for each $i \in \mathbb{I}_1^r$ the system nonlinearities $\mathbf{f}_i(t, \bar{x}_i)$ and $\mathbf{G}_i(t, \bar{x}_i)$ are locally Lipschitz in \bar{x}_i and piece-wise continuous in t , while the intermediate control laws $\mathbf{s}_i(t, \bar{x}_i)$ and $\mathbf{u}(t, \mathbf{x})$ are smooth. Consequently, $\phi(t, \mathbf{z})$ in (C.6) is locally Lipschitz in \mathbf{z} over $\Omega_{\mathbf{z}}$ and piece-wise continuous in t . Thus, by [52, Theorem 54], the existence and uniqueness of a maximal solution $\mathbf{z}(t; \mathbf{z}(0)) \in \Omega_{\mathbf{z}}$ for $t \in [0, \tau_{\max})$ is guaranteed.

Because $\mathbf{z}(t; \mathbf{z}(0)) \in \Omega_{\mathbf{z}}$ for all $t \in [0, \tau_{\max})$, we have $\alpha_h(t; \mathbf{z}(0)) \in (0, \infty)$, $e_s(t; \mathbf{z}(0)) \in (0, \infty)$, and $\hat{e}_i(t; \mathbf{z}(0)) \in (-1, 1)^n$ for all $i \in \mathbb{I}_2^r$ and for all $t \in [0, \tau_{\max})$. Consequently, ε_h in (13), ε_s in (14), and every $\varepsilon_{i,j}$ in (24) (thus $\varepsilon_i \in \mathbb{R}^n$, $i \in \mathbb{I}_2^r$) are well defined on $[0, \tau_{\max})$.

By Assumptions 6, 7, $\alpha_h(t, \mathbf{x}_1)$ has compact level sets with finite positive maxima at each t within $\alpha_h(t, \mathbf{x}_1) > 0$. Let $\alpha_h^*(t) > 0$ denote its finite global maximum and set $b_h := \sup_{\forall t \geq 0} \alpha_h^*(t)$. Then we can infer that $\alpha_h(t, \mathbf{x}_1(t; \mathbf{z}(0))) \in (0, b_h]$ for all $t \in [0, \tau_{\max})$, and the compactness of the corresponding level sets ensures that $\mathbf{x}_1(t) := \mathbf{x}_1(t; \mathbf{z}(0)) \in \mathcal{L}_\infty$ for all $t \in [0, \tau_{\max})$. Similarly, using Assumptions 6, 7, and 9 together with $\alpha_s^*(t) > 0$, and defining $b_s := \sup_{\forall t \geq 0} \alpha_s^*(t)$, leads us to $\alpha_s(t, \mathbf{x}_1(t; \mathbf{z}(0))) \in (0, b_s]$ for all $t \in [0, \tau_{\max})$.

In what follows, function arguments are omitted from the notation when unambiguous. The proof in *Phase II* proceeds through steps corresponding to the controller design stages described in Section 3.3.

Phase II (Step 1): Taking the time derivative of (13) and using (C.3), (C.2), and finally substituting (18), (15)

and (17) yields

$$\begin{aligned}\dot{\varepsilon}_h &= -\varepsilon_h^2 \left[\nabla_{\mathbf{x}_1} \alpha_h^\top \mathbf{f}_1 + \nabla_{\mathbf{x}_1} \alpha_h^\top \mathbf{G}_1 (\Theta_2^{-1} \hat{\mathbf{e}}_2 + \mathbf{s}_1) + \frac{\partial \alpha_h}{\partial t} \right] \\ &= -\varepsilon_h^2 \left[k_s \varepsilon_s^2 \nabla_{\mathbf{x}_1} \alpha_h^\top \mathbf{G}_1 \nabla_{\mathbf{x}_1} \alpha_s + \varphi_h k_h \varepsilon_h^2 \nabla_{\mathbf{x}_1} \alpha_h^\top \mathbf{G}_1 \nabla_{\mathbf{x}_1} \alpha_h \right. \\ &\quad \left. + \sigma_h \right],\end{aligned}\quad (\text{C.7})$$

where $\sigma_h := \nabla_{\mathbf{x}_1} \alpha_h^\top \mathbf{f}_1 + \nabla_{\mathbf{x}_1} \alpha_h^\top \mathbf{G}_1 \Theta_2^{-1} \hat{\mathbf{e}}_2 + \frac{\partial \alpha_h}{\partial t}$. Similarly, taking the time derivative of (14) and using (C.4), (C.2), and then substituting (18), (15), (17), (10) and (16) gives

$$\begin{aligned}\dot{\varepsilon}_s &= -\varepsilon_s^2 \left[\nabla_{\mathbf{x}_1} \alpha_s^\top \mathbf{f}_1 + \nabla_{\mathbf{x}_1} \alpha_s^\top \mathbf{G}_1 (\Theta_2^{-1} \hat{\mathbf{e}}_2 + \mathbf{s}_1) + \frac{\partial \alpha_s}{\partial t} + \dot{\rho}_s \right] \\ &= -\varepsilon_s^2 \left[k_s \varepsilon_s^2 \nabla_{\mathbf{x}_1} \alpha_s^\top \mathbf{G}_1 \nabla_{\mathbf{x}_1} \alpha_s + \varphi_h k_h \varepsilon_h^2 \nabla_{\mathbf{x}_1} \alpha_s^\top \mathbf{G}_1 \nabla_{\mathbf{x}_1} \alpha_h \right. \\ &\quad \left. - \varphi_\gamma \varphi_h k_h \varepsilon_h^2 \nabla_{\mathbf{x}_1} \alpha_s^\top \mathbf{G}_1 \nabla_{\mathbf{x}_1} \alpha_h + \sigma_s \right],\end{aligned}\quad (\text{C.8})$$

where $\sigma_s := \nabla_{\mathbf{x}_1} \alpha_s^\top \mathbf{f}_1 + \nabla_{\mathbf{x}_1} \alpha_s^\top \mathbf{G}_1 \Theta_2^{-1} \hat{\mathbf{e}}_2 + \frac{\partial \alpha_s}{\partial t} + \dot{\rho}_s^{\text{n}} - k_r \rho_s^{\text{r}}$.

From *Phase I*, $\mathbf{x}_1(t) \in \mathcal{L}_\infty$, $\forall t \in [0, \tau_{\max}]$. Therefore, by the continuity of $\mathbf{f}_1(t, \mathbf{x}_1)$ and $\mathbf{G}_1(t, \mathbf{x}_1)$ in \mathbf{x}_1 and Assumption 2, both $\mathbf{f}_1(t, \mathbf{x}_1)$ and $\mathbf{G}_1(t, \mathbf{x}_1)$ remain bounded $\forall t \in [0, \tau_{\max}]$. Moreover, from the expressions of $\nabla_{\mathbf{x}_1} \alpha_s(t, \mathbf{x}_1)$, $\nabla_{\mathbf{x}_1} \alpha_h(t, \mathbf{x}_1)$, $\frac{\partial \alpha_s(t, \mathbf{x}_1)}{\partial t}$, and $\frac{\partial \alpha_h(t, \mathbf{x}_1)}{\partial t}$ in Appendix B, their continuity in \mathbf{x}_1 , and Assumptions 4 and 5, conclude $\nabla_{\mathbf{x}_1} \alpha_s(t, \mathbf{x}_1)$, $\nabla_{\mathbf{x}_1} \alpha_h(t, \mathbf{x}_1)$, $\frac{\partial \alpha_s(t, \mathbf{x}_1)}{\partial t}$, $\frac{\partial \alpha_h(t, \mathbf{x}_1)}{\partial t} \in \mathcal{L}_\infty$, $\forall t \in [0, \tau_{\max}]$. Additionally, by construction we have $\Theta_2^{-1}(t), \dot{\rho}_s^{\text{n}}(t) \in \mathcal{L}_\infty$, $\forall t \geq 0$, and $\hat{\mathbf{e}}_2 \in \mathcal{L}_\infty$, $\forall t \in [0, \tau_{\max}]$ by *Phase I*. Collectively, these facts show that $\sigma_h \in \mathcal{L}_\infty$ in (C.7) for all $t \in [0, \tau_{\max}]$. Similarly, one can verify that $\sigma_s \in \mathcal{L}_\infty$ in (C.8) for all $t \in [0, \tau_{\max}]$ if $\rho_s^{\text{r}}(t) \in \mathcal{L}_\infty$.

Recall that (7) and (8) hold iff ε_h and ε_s in (13) and (14) remain bounded. We now demonstrate that $\varepsilon_h, \varepsilon_s \in \mathcal{L}_\infty$ for all $t \in [0, \tau_{\max}]$, which in turn guarantees that both $\mathbf{s}_1(t, \mathbf{x})$ in (18) and its derivative remain bounded for all $t \in [0, \tau_{\max}]$. To do so, we shall establish the boundedness of ε_h and ε_s for each following modes of the smooth switch functions φ_h and φ_γ :

- (A) When $\varphi_h(t) = 0$, i.e., when $\mathbf{x}_1(t)$ evolves in the interior region $\Omega_h^{\text{ir}}(t)$ defined in (28a)
- (B) When $\varphi_h(t) > 0$, i.e., when $\mathbf{x}_1(t)$ evolves in the boundary region $\Omega_h^{\text{br}}(t)$ defined in (28b), with:
 - (B1) $\varphi_\gamma(t) = 0$ (i.e., the virtual relaxation of soft constraints is inactive).
 - (B2) $\varphi_\gamma(t) > 0$ (i.e., the virtual relaxation of soft constraints is active).

Throughout, let $\mathcal{I}_A, \mathcal{I}_{B1}, \mathcal{I}_{B2} \subseteq [0, \tau_{\max}]$ denote the time intervals during which modes *A*, *B1*, and *B2* are active, respectively. Observe that $\mathcal{I}_A \cup \mathcal{I}_{B1} \cup \mathcal{I}_{B2} = [0, \tau_{\max}]$ and that each interval may consist of several disjoint sub-intervals.

Mode A ($\varphi_h(t) = 0$): Based on Assumption 7, for a sufficiently small $\delta_h > 0$, $\Omega_h^{\text{ir}}(t)$ in (28a) is non-empty. When

Mode A is active we have $t \in \mathcal{I}_A$. In this scenario, since $\alpha_h(t, \mathbf{x}_1) \geq \delta_h$ is strictly above zero $\forall t \in \mathcal{I}_A$, from (13) we have $\varepsilon_h \in \mathcal{L}_\infty$, $\forall t \in \mathcal{I}_A$. Consequently, there exists a $\bar{\varepsilon}_h^A > 0$ such that $0 < \varepsilon_h < \bar{\varepsilon}_h^A$, $\forall t \in \mathcal{I}_A$. It remains to show that $\varepsilon_s \in \mathcal{L}_\infty$ whenever $\varphi_h(t) = 0$. To this end, we first show that σ_s in (C.8) is bounded $\forall t \in \mathcal{I}_A$ and then use proof-by-contradiction to establish $\varepsilon_s \in \mathcal{L}_\infty$, $\forall t \in \mathcal{I}_A$.

Note that since $\varphi_h(t) = 0$, from (16) we have $\dot{\rho}_s^{\text{r}} = -k_r \rho_s^{\text{r}}$, which implies that $\rho_s^{\text{r}} \in \mathcal{L}_\infty$, $\forall t \in \mathcal{I}_A$. Hence, followed by the arguments below (C.8), $\sigma_s \in \mathcal{L}_\infty$, $\forall t \in \mathcal{I}_A$.

From *Phase I*, we have $e_s(t) \in (0, +\infty)$ for all $t \in [0, \tau_{\max}]$; thus, from (14), ε_s can only diverge upward, i.e., $\varepsilon_s \rightarrow +\infty$. Suppose $\varepsilon_s(t) \rightarrow +\infty$ as $t \rightarrow t'$ for some $t' \in \mathcal{I}_A$ with $\varphi_h(t') = 0$. Since $\varphi_h = 0$, (C.8) becomes $\dot{\varepsilon}_s = -\varepsilon_s^2 (k_s \varepsilon_s^2 \nabla_{\mathbf{x}_1} \alpha_s^\top \mathbf{G}_1 \nabla_{\mathbf{x}_1} \alpha_s + \sigma_s)$. Given that the quadratic term $\nabla_{\mathbf{x}_1} \alpha_s^\top \mathbf{G}_1 \nabla_{\mathbf{x}_1} \alpha_s$ is positive definite (Assumption 1) and σ_s is bounded, if $\nabla_{\mathbf{x}_1} \alpha_s \neq 0$ then $\dot{\varepsilon}_s \rightarrow -\infty$ as $t \rightarrow t'$, contradicting $\varepsilon_s(t) \rightarrow +\infty$. Moreover, by Assumption 9, $\nabla_{\mathbf{x}_1} \alpha_s = 0$ occurs only when $\mathbf{x}_1(t)$ lies inside $\Omega_s(t)$, i.e., when $\alpha_s(t, \mathbf{x}_1(t)) > 0$, for which $e_s(t) > 0$ holds by construction of $\rho_s(t) \leq 0$ in (12). Thus, $\nabla_{\mathbf{x}_1} \alpha_s = 0$ guarantees that ε_s is bounded, again contradicting the occurrence of $\varepsilon_s(t) \rightarrow +\infty$. Overall, ε_s remains bounded for all $t \in \mathcal{I}_A$. Therefore, there exists a $\bar{\varepsilon}_s^A > 0$ such that $0 < \varepsilon_s \leq \bar{\varepsilon}_s^A$ for all $t \in \mathcal{I}_A$ whenever $\varphi_h(t) = 0$.

Mode B1 ($\varphi_h(t) > 0 \ \& \ \varphi_\gamma(t) = 0$): Under this mode we have $t \in \mathcal{I}_{B1}$. By definition of the smooth switch function, $\varphi_\gamma = 0$ iff $\gamma = \varepsilon_h \nabla_{\mathbf{x}_1} \alpha_s^\top \mathbf{G}_1 \nabla_{\mathbf{x}_1} \alpha_h \geq 0$. From *Phase I* we know $\varepsilon_h > 0$, $\forall t \in [0, \tau_{\max}]$, hence, $\nabla_{\mathbf{x}_1} \alpha_s^\top \mathbf{G}_1 \nabla_{\mathbf{x}_1} \alpha_h \geq 0$ whenever *Mode B1* is active. Unlike *Mode A*, here $\alpha_h(t, \mathbf{x}_1) < \delta_h$, so ε_h in (13) could grow unbounded, leading to the violation of hard constraints. Below, we prove by contradiction that $\varepsilon_h, \varepsilon_s \in \mathcal{L}_\infty$ on \mathcal{I}_{B1} .

Recall that since $\varepsilon_h > 0$ for all $t \in [0, \tau_{\max}]$, ε_h can only grow unbounded from above. Therefore, suppose $\varepsilon_h \rightarrow +\infty$ as $t \rightarrow t'$ for some $t' \in \mathcal{I}_{B1}$. Since $\sigma_h \in \mathcal{L}_\infty$ and $\nabla_{\mathbf{x}_1} \alpha_s^\top \mathbf{G}_1 \nabla_{\mathbf{x}_1} \alpha_h \geq 0$, if $\nabla_{\mathbf{x}_1} \alpha_h \neq 0$ the bracketed term on the RHS of (C.7) stays positive, so $\dot{\varepsilon}_h \rightarrow -\infty$, contradicting $\varepsilon_h \rightarrow +\infty$. Furthermore, by Assumption 11, we can have $\nabla_{\mathbf{x}_1} \alpha_h = 0$ only when $\alpha_h(t, \mathbf{x}_1) > 0$. From (14) it then follows that $\varepsilon_h \in \mathcal{L}_\infty$ whenever $\nabla_{\mathbf{x}_1} \alpha_h = 0$, which again contradicts with $\varepsilon_h \rightarrow +\infty$.

Overall, we have $\varepsilon_h \in \mathcal{L}_\infty$ on \mathcal{I}_{B1} , so there exists a $\bar{\varepsilon}_h^{B1} > 0$ with $0 < \varepsilon_h < \bar{\varepsilon}_h^{B1}$ for all $t \in \mathcal{I}_{B1}$.

Since $\varphi_\gamma(t) = 0$, (16) yields $\dot{\rho}_s^{\text{r}} = -k_r \rho_s^{\text{r}}$ so $\rho_s^{\text{r}} \in \mathcal{L}_\infty$ on \mathcal{I}_{B1} . By the arguments below (C.8), this also gives $\sigma_s \in \mathcal{L}_\infty$, $\forall t \in \mathcal{I}_{B1}$. Moreover, recall that $e_s(t) \in (0, +\infty)$, $\forall t \in [0, \tau_{\max}]$ and thus ε_s can only diverge upward. Now suppose $\varepsilon_s \rightarrow +\infty$ as $t \rightarrow t'$ for some $t' \in \mathcal{I}_{B1}$. Since $\sigma_s, \varepsilon_h \in \mathcal{L}_\infty$, $\varphi_\gamma = 0$, and $\nabla_{\mathbf{x}_1} \alpha_s^\top \mathbf{G}_1 \nabla_{\mathbf{x}_1} \alpha_h \geq 0$, if $\nabla_{\mathbf{x}_1} \alpha_h \neq 0$ the bracketed term on the RHS of (C.8) remains positive, so $\dot{\varepsilon}_s \rightarrow -\infty$, contradicting $\varepsilon_s \rightarrow +\infty$. In addition, under Assumption 9, similarly to *Mode A* one can conclude that $\nabla_{\mathbf{x}_1} \alpha_s = 0$ ensures the boundedness of ε_s , contradicting $\varepsilon_s \rightarrow +\infty$. Hence, $\varepsilon_s \in \mathcal{L}_\infty$ on \mathcal{I}_{B1} , and there exists a $\bar{\varepsilon}_s^{B1} > 0$ such that $0 < \varepsilon_s \leq \bar{\varepsilon}_s^{B1}$, $\forall t \in \mathcal{I}_{B1}$.

Mode B2 ($\varphi_h(t) > 0 \ \& \ \varphi_\gamma(t) > 0$): In this mode we

have $t \in \mathcal{I}_{B2}$. Moreover, since $\varphi_\gamma > 0$ it holds that $\gamma = \varepsilon_h \nabla_{\mathbf{x}_1} \alpha_s^\top \mathbf{G}_1 \nabla_{\mathbf{x}_1} \alpha_h < 0$. Consequently, as $\varepsilon_h > 0$ for all $t \in [0, \tau_{\max}]$, we have $\nabla_{\mathbf{x}_1} \alpha_s^\top \mathbf{G}_1 \nabla_{\mathbf{x}_1} \alpha_h < 0$ whenever *Mode B2* is active. We shall use proof-by-contradiction to establish $\varepsilon_h, \varepsilon_s \in \mathcal{L}_\infty$ for all $t \in \mathcal{I}_{B2}$.

From (14), letting $\varepsilon_s \rightarrow +\infty$ gives $e_s = \alpha_s(t, \mathbf{x}_1(t)) - (\rho_s^u(t) - \rho_s^r(t)) \rightarrow 0$. Since $\rho_s^u(t) \in \mathcal{L}_\infty$, $\forall t \geq 0$ and, by *Phase I*, $\alpha_s(t, \mathbf{x}_1(t)) \in \mathcal{L}_\infty$, $\forall t \in [0, \tau_{\max}]$, it follows that $\rho_s^r(t)$, and thus σ_s in (C.8) remains bounded as $\varepsilon_s \rightarrow +\infty$.

Moreover, with $\gamma = \varepsilon_h \nabla_{\mathbf{x}_1} \alpha_s^\top \mathbf{G}_1 \nabla_{\mathbf{x}_1} \alpha_h$ and $\nabla_{\mathbf{x}_1} \alpha_s^\top \mathbf{G}_1 \nabla_{\mathbf{x}_1} \alpha_h < 0$, γ becomes arbitrarily negative for large ε_h . Because the smooth switch is defined by $\varphi_\gamma := \varphi(\gamma, 0, -\delta_\gamma)$ with fixed $\delta_\gamma > 0$, we have $\varphi_\gamma(t) = 1$ whenever ε_h is sufficiently large (i.e, when $\varepsilon_h \rightarrow +\infty$).

Suppose both $\varepsilon_s, \varepsilon_h \rightarrow +\infty$ as $t \rightarrow t'$ for some $t' \in \mathcal{I}_{B2}$. Because $\varphi_\gamma(t) = 1$ and $\sigma_s \in \mathcal{L}_\infty$, the RHS of (C.8) implies that $\varepsilon_s \rightarrow -\infty$ whenever $\nabla_{\mathbf{x}_1} \alpha_s \neq 0$. This contradicts our assumption, so ε_s and ε_h cannot diverge simultaneously. Next, assume $\varepsilon_s \rightarrow +\infty$ while $\varepsilon_h \in \mathcal{L}_\infty$. The RHS of (C.8) again forces $\varepsilon_s \rightarrow -\infty$ when $\nabla_{\mathbf{x}_1} \alpha_s \neq 0$, contradicting $\varepsilon_s \rightarrow +\infty$. Conversely, if $\varepsilon_h \rightarrow +\infty$ while $\varepsilon_s \in \mathcal{L}_\infty$, the RHS of (C.7) yields $\varepsilon_h \rightarrow -\infty$ whenever $\nabla_{\mathbf{x}_1} \alpha_h \neq 0$, which is likewise contradictory. Similarly to the discussions provided in the analysis of previous modes one can claim that ε_s and ε_h remain bounded when $\nabla_{\mathbf{x}_1} \alpha_s = 0$ and $\nabla_{\mathbf{x}_1} \alpha_h = 0$, respectively. Hence we conclude $\varepsilon_s, \varepsilon_h \in \mathcal{L}_\infty$ for all $t \in \mathcal{I}_{B2}$. Therefore, constants $\bar{\varepsilon}_h^{B2} > 0$ and $\bar{\varepsilon}_s^{B2} > 0$ exist such that $0 < \varepsilon_h \leq \bar{\varepsilon}_h^{B2}$, $0 < \varepsilon_s \leq \bar{\varepsilon}_s^{B2}$, $\forall t \in \mathcal{I}_{B2}$.

Define $\bar{\varepsilon}_s := \max\{\bar{\varepsilon}_s^A, \bar{\varepsilon}_s^{B1}, \bar{\varepsilon}_s^{B2}\}$ and $\bar{\varepsilon}_h := \max\{\bar{\varepsilon}_h^A, \bar{\varepsilon}_h^{B1}, \bar{\varepsilon}_h^{B2}\}$, which are independent of τ_{\max} . Now combining all the results from *Modes A*, *B1*, and *B2* gives

$$0 < \varepsilon_s \leq \bar{\varepsilon}_s, \quad \text{and} \quad 0 < \varepsilon_h \leq \bar{\varepsilon}_h, \quad \forall t \in [0, \tau_{\max}). \quad (\text{C.9})$$

Recall that when *Modes A* and *B1* are active we have already shown that $\rho_s^r(t) \in \mathcal{L}_\infty$. Moreover, when *Mode B2* is active we proved that $\varepsilon_s, \varepsilon_h \in \mathcal{L}_\infty$. As a result, using (C.9) and Lemma 1 in Appendix D, we can conclude that $\rho_s^r(t) \in \mathcal{L}_\infty$ and $\rho_s^r(t) \geq 0$, $\forall t \in [0, \tau_{\max}]$. Hence, there exists a constant $\bar{\rho}_s^r > 0$, independent of τ_{\max} , such that

$$0 \leq \rho_s^r(t) \leq \bar{\rho}_s^r, \quad \forall t \in [0, \tau_{\max}). \quad (\text{C.10})$$

Combining (13), (14), (C.9), (C.10), and the *Phase I* results yields, for all $t \in [0, \tau_{\max}]$, that

$$\frac{1}{\bar{\varepsilon}_h} \leq \alpha_h(t, \mathbf{x}_1(t)) \leq b_h, \quad \text{and} \quad \frac{1}{\bar{\varepsilon}_s} \leq \alpha_s(t, \mathbf{x}_1(t)) \leq b_s, \quad (\text{C.11})$$

where b_h and b_s are constant defined in *Phase I*. Because $\rho_0 \leq 0$ in (11), from (12), (C.11), and (C.10) we obtain

$$0 < \frac{1}{\bar{\varepsilon}_s} - \rho_0 \leq e_s(t, \mathbf{x}_1(t)) \leq b_s + \bar{\rho}_s^r, \quad \forall t \in [0, \tau_{\max}). \quad (\text{C.12})$$

Finally, by (C.9) and the boundedness of $\nabla \alpha_h(t, \mathbf{x}_1)$ and $\nabla \alpha_s(t, \mathbf{x}_1)$, $\forall t \in [0, \tau_{\max}]$, the first intermediate control signal $\mathbf{s}_1(t, \mathbf{x}_1)$ in (18) is bounded $\forall t \in [0, \tau_{\max}]$. Additionally, using the aforementioned results, it is not difficult to verify that $\dot{\mathbf{s}}_1(t, \mathbf{x}_1)$ is likewise bounded $\forall t \in [0, \tau_{\max}]$.

Phase II (Step 2 $\leq i \leq r$): Differentiating $\varepsilon_i = \text{col}(\varepsilon_{i,j})$ with respect to time and using (24), (19), (1), and (C.1) gives

$$\begin{aligned} \dot{\varepsilon}_i &= \Xi_i \left[\mathbf{f}_i(t, \mathbf{x}_1, \hat{\mathbf{e}}_2, \dots, \hat{\mathbf{e}}_i) + \mathbf{G}_i(t, \mathbf{x}_1, \hat{\mathbf{e}}_2, \dots, \hat{\mathbf{e}}_i) \right. \\ &\quad \times \left(\boldsymbol{\Theta}_{i+1}^{-1} \hat{\mathbf{e}}_{i+1} + \mathbf{s}_i(t, \mathbf{x}_1, \hat{\mathbf{e}}_2, \dots, \hat{\mathbf{e}}_i) \right) \\ &\quad \left. - \dot{\mathbf{s}}_{i-1}(t, \mathbf{x}_1, \hat{\mathbf{e}}_2, \dots, \hat{\mathbf{e}}_{i-1}) - \dot{\boldsymbol{\Theta}}_i \hat{\mathbf{e}}_i \right], \quad i \in \mathbb{I}_2^{r-1}, \end{aligned} \quad (\text{C.13})$$

where for $i = r$, the term $\boldsymbol{\Theta}_{i+1}^{-1} \hat{\mathbf{e}}_{i+1} + \mathbf{s}_i$ should be replaced by \mathbf{u} in (27). Recall that, $\boldsymbol{\Theta}_i := \text{diag}(\vartheta_{i,j})$ and $\Xi_i := \text{diag}(\xi_{i,j})$, in which $\xi_{i,j}$ are given in (26).

The rest of the proof in *Phase II* continues similarly to steps 2 to r of Theorem 1's proof in [32]. Therefore for brevity we only provide the proof sketch in the following. For each step $i = 2, \dots, r$, we consider barrier functions $V_i(\varepsilon_i) = \frac{1}{2} \varepsilon_i^\top \varepsilon_i$ as a positive definite and radially unbounded Lyapunov function candidate with respect to ε_i . Then using the results in *Phase I*, Assumptions 2, 3, and the boundedness of $\mathbf{s}_{i-1}(t, \mathbf{x}_1, \hat{\mathbf{e}}_2, \dots, \hat{\mathbf{e}}_{i-1})$, $\dot{\mathbf{s}}_{i-1}(t, \mathbf{x}_1, \hat{\mathbf{e}}_2, \dots, \hat{\mathbf{e}}_{i-1})$, $\forall t \in [0, \tau_{\max}]$, established in the previous step, and following standard Lyapunov analysis we can show that ε_i is Uniformly Ultimately Bounded (UUB) [53]. Therefore, there exists $\bar{\varepsilon}_i > 0$ such that $\|\varepsilon_i\| < \bar{\varepsilon}_i$, $\forall t \in [0, \tau_{\max}]$. Hence, from the inverse logarithmic transformation in (24), we get

$$-1 < \frac{e^{-\bar{\varepsilon}_i} - 1}{e^{-\bar{\varepsilon}_i} + 1} =: -\varsigma_{i,j} \leq \hat{\varepsilon}_{i,j}(t) \leq \varsigma_{i,j} := \frac{e^{\bar{\varepsilon}_i} - 1}{e^{\bar{\varepsilon}_i} + 1} < 1. \quad (\text{C.14})$$

Moreover, at each step one can establish $\mathbf{s}_i(t, \mathbf{x}_1, \hat{\mathbf{e}}_2, \dots, \hat{\mathbf{e}}_i)$, $\dot{\mathbf{s}}_i(t, \mathbf{x}_1, \hat{\mathbf{e}}_2, \dots, \hat{\mathbf{e}}_i) \in \mathcal{L}_\infty$, $\forall t \in [0, \tau_{\max}]$.

As a result, by proceeding recursively, we can show that all intermediate control signals \mathbf{s}_i and the control law \mathbf{u} remain bounded $\forall t \in [0, \tau_{\max}]$. Furthermore, from (C.1) and the results established so far, it follows that all system states \mathbf{x}_i , $i = \mathbb{I}_1^{r-1}$, are also bounded for all $t \in [0, \tau_{\max}]$.

Phase III: To prove that $\tau_{\max} = \infty$, first collect the bounds in (C.10), (C.11), (C.12), and (C.14), and define

$$\Omega'_{\alpha_h} := [\frac{1}{\bar{\varepsilon}_h}, b_h], \quad (\text{C.15a})$$

$$\Omega'_{e_s} := [\frac{1}{\bar{\varepsilon}_s} - \rho_0, b_s + \bar{\rho}_s^r], \quad (\text{C.15b})$$

$$\Omega'_{\rho_s^r} := [0, \bar{\rho}_s^r], \quad (\text{C.15c})$$

$$\Omega'_{\hat{\mathbf{e}}_i} := [-\varsigma_{i,1}, \varsigma_{i,1}] \times \dots \times [-\varsigma_{i,n}, \varsigma_{i,n}], \quad i \in \mathbb{I}_2^r, \quad (\text{C.15d})$$

$$\Omega'_{\hat{\mathbf{e}}} := \Omega'_{\hat{\mathbf{e}}_2} \times \dots \times \Omega'_{\hat{\mathbf{e}}_r} \subset (-1, 1)^n \times \dots \times (-1, 1)^n. \quad (\text{C.15e})$$

Next, owing to the compactness of the level sets of $\alpha_h(t, \mathbf{x}_1)$ and the bounds in (C.11), we have $\mathbf{x}_1(t) \in \Omega'_{\mathbf{x}_1}(t) \subset \mathbb{R}^n$, $\forall t \in [0, \tau_{\max}]$, where

$$\Omega'_{\mathbf{x}_1}(t) := \{\mathbf{x}_1 \in \mathbb{R}^n \mid \frac{1}{\bar{\varepsilon}_h} \leq \alpha_h(t, \mathbf{x}_1) \leq b_h\}. \quad (\text{C.16})$$

Define the time-invariant super-set $\Omega_{\mathbf{x}_1}^{s'} := \bigcup_{t=0}^{+\infty} \Omega'_{\mathbf{x}_1}(t) \subset \mathbb{R}^n$. Then we have $\mathbf{x}_1(t) \in \Omega_{\mathbf{x}_1}^{s'} \subset \mathbb{R}^n$ for all $t \in [0, \tau_{\max}]$.

Finally, define $\Omega'_{\mathbf{z}} := \Omega_{\mathbf{x}_1}^{s'} \times \Omega'_{\alpha_h} \times \Omega'_{\rho_s^r} \times \Omega'_{e_s} \times \Omega'_{\hat{\mathbf{e}}}$, which is a non-empty compact subset of $\Omega_{\mathbf{z}}$. Recall that

results established in *Phase I* and *Phase II* ensure that $\mathbf{z}(t; \mathbf{z}(0)) \in \Omega'_{\mathbf{z}}, \forall t \in [0, \tau_{\max}]$. Assume, for contradiction, that $\tau_{\max} < \infty$. Because $\Omega'_{\mathbf{z}} \subset \Omega_{\mathbf{z}}$, Proposition C.3.6 of [52, p. 481] implies the existence of a time $t' \in [0, \tau_{\max})$ such that $\mathbf{z}(t'; \mathbf{z}(0)) \notin \Omega'_{\mathbf{z}}$, contradicting the previous inclusion. Hence $\tau_{\max} = \infty$. Consequently, every closed-loop control signal remains bounded $\forall t \geq 0$. Moreover, since $\alpha_h(t, \mathbf{x}_1(t)) \in [\frac{1}{\varepsilon_h}, b_h] \subset (0, +\infty)$ and $\varepsilon_s(t, \mathbf{x}_1(t)) \in [\frac{1}{\varepsilon_s} - \rho_0, b_s + \bar{\rho}_s^r] \subset (0, +\infty)$, $\forall t \geq 0$, conditions (7) and (8) are satisfied for all time. Therefore, the time-varying set $\Omega_h(t) \cap \tilde{\Omega}_s(t)$ is forward invariant, completing the proof. \square

Appendix D. On Properties of $\rho_s^r(t)$

The following lemma gives two useful properties of $\rho_s^r(t)$.

Lemma 1. *The relaxation signal $\rho_s^r(t)$ governed by (16) satisfies $\rho_s^r(t) \geq 0$ for all $t \geq 0$. Furthermore, if $\varepsilon_h \in \mathcal{L}_\infty$ and $\varepsilon_h > 0$ hold, then $\rho_s^r \in \mathcal{L}_\infty$.*

Proof. Note that whenever $\varphi_h(t) = 0$ or $\varphi_\gamma(t) = 0$, the first term on the RHS of (16) vanishes. When $\varphi_h(t) > 0$ and $\varphi_\gamma(t) > 0$, combining (16) with (15) gives

$$\dot{\rho}_s^r = -\varphi_\gamma \varphi_h k_h \varepsilon_h^2 \nabla_{\mathbf{x}_1} \alpha_s^\top \mathbf{G}_1 \nabla_{\mathbf{x}_1} \alpha_h - k_r \rho_s^r,$$

where $\nabla_{\mathbf{x}_1} \alpha_s^\top \mathbf{G}_1 \nabla_{\mathbf{x}_1} \alpha_h < 0$, $k_h > 0$, and $\varepsilon_h > 0$. As a result, the first term on the RHS of $\dot{\rho}_s^r$ is always non-negative.

Let $t' \in [0, \infty)$ be an arbitrary time instant. If $\rho_s^r(t') = 0$, then $\dot{\rho}_s^r(t') > 0$, implying $\rho_s^r(t) \geq 0$ for all $t \geq t'$. Setting $t' = 0$ yields $\rho_s^r(t) \geq 0$ for all $t \geq 0$ provided that the solution of (16) exists.

Because $\varepsilon_h > 0$ and $\varepsilon_h \in \mathcal{L}_\infty$, (13) ensures $\alpha_h(t, \mathbf{x}_1) > 0$. Moreover, recall that $\alpha_h(t, \mathbf{x}_1)$ has compact level sets (Assumption 6) and satisfies $\alpha_h(t, \mathbf{x}_1) \leq \alpha_s^*(t) := \max_{\mathbf{x}_1 \in \mathbb{R}^n} \alpha_h(t, \mathbf{x}_1)$, where $\alpha_s^*(t)$ is finite and positive (Assumption 7). Thus $\alpha_h(t, \mathbf{x}_1) > 0$ implies that \mathbf{x}_1 is bounded. Owing to Assumptions 2, 5, 4, boundedness of \mathbf{x}_1 , and continuity of $\nabla_{\mathbf{x}_1} \alpha_s(t, \mathbf{x}_1)$, $\mathbf{G}_1(t, \mathbf{x}_1)$, and $\nabla_{\mathbf{x}_1} \alpha_h(t, \mathbf{x}_1)$, all these terms are bounded. Consequently, if $\varepsilon_h > 0$ and $\varepsilon_h \in \mathcal{L}_\infty$, the first term on the RHS of (16) is always bounded and non-negative.

Finally, assume $\rho_s^r(t) \rightarrow +\infty$. Then the RHS of (16) implies $\dot{\rho}_s^r(t) \rightarrow -\infty$, contradicting $\rho_s^r(t) \rightarrow +\infty$. Hence, provided that $\varepsilon_h > 0$ and $\varepsilon_h \in \mathcal{L}_\infty$, $\rho_s^r(t)$ remains bounded. \square

References

- [1] D. Q. Mayne, Model predictive control: Recent developments and future promise, *Automatica* 50 (12) (2014) 2967–2986.
- [2] E. Garone, S. Di Cairano, I. Kolmanovsky, Reference and command governors for systems with constraints: A survey on theory and applications, *Automatica* 75 (2017) 306–328.
- [3] M. M. Nicotra, E. Garone, The explicit reference governor: A general framework for the closed-form control of constrained nonlinear systems, *IEEE Control Systems Magazine* 38 (4) (2018) 89–107.
- [4] A. D. Ames, X. Xu, J. W. Grizzle, P. Tabuada, Control barrier function based quadratic programs for safety critical systems, *IEEE Transactions on Automatic Control* 62 (8) (2016) 3861–3876.
- [5] K. P. Tee, S. S. Ge, E. H. Tay, Barrier lyapunov functions for the control of output-constrained nonlinear systems, *Automatica* 45 (4) (2009) 918–927.
- [6] K. P. Tee, B. Ren, S. S. Ge, Control of nonlinear systems with time-varying output constraints, *Automatica* 47 (11) (2011) 2511–2516.
- [7] A. Ilchmann, E. P. Ryan, C. J. Sangwin, Tracking with prescribed transient behaviour, *ESAIM: Control, Optimisation and Calculus of Variations* 7 (2002) 471–493.
- [8] C. P. Bechlioulis, G. A. Rovithakis, Robust adaptive control of feedback linearizable mimo nonlinear systems with prescribed performance, *IEEE Transactions on Automatic Control* 53 (9) (2008) 2090–2099.
- [9] X. Jin, Adaptive fixed-time control for mimo nonlinear systems with asymmetric output constraints using universal barrier functions, *IEEE Transactions on Automatic Control* 64 (7) (2018) 3046–3053.
- [10] C. P. Bechlioulis, G. A. Rovithakis, A low-complexity global approximation-free control scheme with prescribed performance for unknown pure feedback systems, *Automatica* 50 (4) (2014) 1217–1226.
- [11] T. Berger, H. H. Lê, T. Reis, Funnel control for nonlinear systems with known strict relative degree, *Automatica* 87 (2018) 345–357.
- [12] Funnel control — a survey, *Annual Reviews in Control* 60 (2025) 101024.
- [13] M. N. Zeilinger, M. Morari, C. N. Jones, Soft constrained model predictive control with robust stability guarantees, *IEEE Transactions on Automatic Control* 59 (5) (2014) 1190–1202.
- [14] A. D. Ames, S. Coogan, M. Egerstedt, G. Notomista, K. Sreenath, P. Tabuada, Control barrier functions: Theory and applications, in: 2019 18th European control conference (ECC), IEEE, 2019, pp. 3420–3431.
- [15] R. Ji, B. Yang, J. Ma, S. S. Ge, Saturation-tolerant prescribed control for a class of mimo nonlinear systems, *IEEE Transactions on Cybernetics* 52 (12) (2021) 13012–13026.

[16] F. Fotiadis, G. A. Rovithakis, Input-constrained prescribed performance control for high-order mimo uncertain nonlinear systems via reference modification, *IEEE Transactions on Automatic Control* (2023).

[17] P. S. Trakas, C. P. Bechlioulis, Robust adaptive prescribed performance control for unknown nonlinear systems with input amplitude and rate constraints, *IEEE Control Systems Letters* (2023).

[18] P. S. Trakas, V. Modugno, D. Kanoulas, C. P. Bechlioulis, Input-output constrained adaptive cruise control, *IEEE Transactions on Control Systems Technology* (2025).

[19] J. Lei, T. Meng, Y. Zhu, K. Wang, W. Wang, Adaptive constrained attitude control of spacecraft with compatible and guaranteed performance, *IEEE Transactions on Aerospace and Electronic Systems* 60 (2) (2024) 2193–2209.

[20] Z. Yin, J. Luo, C. Wei, Robust prescribed performance control for euler-lagrange systems with practically finite-time stability, *European Journal of Control* 52 (2020) 1–10.

[21] H. Yang, Y. Wang, Y. Song, Z. Shao, Finite-gain based adaptive predefined-time control for a class of strict-feedback systems subject to output constraints, *Automatica* 173 (2025) 112072.

[22] R. Ji, D. Li, S. S. Ge, H. Li, Tunnel prescribed control of nonlinear systems with unknown control directions, *IEEE transactions on neural networks and learning systems* (2023).

[23] Y. Shi, B. Yi, W. Xie, W. Zhang, Enhancing prescribed performance of tracking control using monotone tube boundaries, *Automatica* 159 (2024) 111304.

[24] X. Bu, Prescribed performance control approaches, applications and challenges: A comprehensive survey, *Asian Journal of Control* (2022).

[25] L. Sun, Y. Song, Global tracking control with tunable transient performance under deferred time-varying constraints, *IEEE Transactions on Systems, Man, and Cybernetics: Systems* (2024).

[26] Y.-D. Song, S. Zhou, Tracking control of uncertain nonlinear systems with deferred asymmetric time-varying full state constraints, *Automatica* 98 (2018) 314–322.

[27] L. Kong, W. He, Z. Liu, X. Yu, C. Silvestre, Adaptive tracking control with global performance for output-constrained mimo nonlinear systems, *IEEE Transactions on Automatic Control* 68 (6) (2022) 3760–3767.

[28] Z. Shao, Y. Wang, D. Luo, Y. Song, A unified approach for tracking control of mimo nonlinear systems under unknown control directions and irregular constraints, *IEEE Transactions on Automation Science and Engineering* 21 (4) (2023) 6845–6854.

[29] K. Zhao, Y. Song, Decision function-based adaptive control of uncertain systems subject to irregular output constraints, *IEEE Transactions on Automatic Control* 69 (11) (2024) 8026–8033.

[30] T. Berger, A. Ilchmann, E. P. Ryan, Funnel control of nonlinear systems, *Mathematics of Control, Signals, and Systems* 33 (1) (2021) 151–194.

[31] F. Mehdifar, L. Lindemann, C. P. Bechlioulis, D. V. Dimarogonas, Control of nonlinear systems under multiple time-varying output constraints: A single funnel approach, in: 2023 62nd IEEE Conference on Decision and Control (CDC), IEEE, 2023, pp. 6743–6748.

[32] F. Mehdifar, L. Lindemann, C. P. Bechlioulis, D. V. Dimarogonas, Low-complexity control for a class of uncertain mimo nonlinear systems under generalized time-varying output constraints, *IEEE Transactions on Automatic Control* (2024) 1–16.

[33] F. Mehdifar, C. P. Bechlioulis, F. Hashemzadeh, M. Baradarannia, Prescribed performance distance-based formation control of multi-agent systems, *Automatica* 119 (2020) 109086.

[34] S.-L. Dai, K. Lu, X. Jin, Fixed-time formation control of unicycle-type mobile robots with visibility and performance constraints, *IEEE Transactions on Industrial Electronics* 68 (12) (2020) 12615–12625.

[35] C. K. Verginis, A. Nikou, D. V. Dimarogonas, Robust formation control in se (3) for tree-graph structures with prescribed transient and steady state performance, *Automatica* 103 (2019) 538–548.

[36] C. K. Verginis, C. P. Bechlioulis, D. V. Dimarogonas, K. J. Kyriakopoulos, Robust distributed control protocols for large vehicular platoons with prescribed transient and steady-state performance, *IEEE Transactions on Control Systems Technology* 26 (1) (2017) 299–304.

[37] C. P. Bechlioulis, S. Heshmati-Alamdar, G. C. Karatas, K. J. Kyriakopoulos, Robust image-based visual servoing with prescribed performance under field of view constraints, *IEEE Transactions on Robotics* 35 (4) (2019) 1063–1070.

[38] L. Zhu, L. Zhang, C. Qian, C. Hua, Improved safe tracking error-constrained control for unknown interconnected time-delay nonlinear systems with discontinuous references, *IEEE Transactions on Cybernetics* (2025).

[39] F. Mehdifar, C. P. Bechlioulis, D. V. Dimarogonas, Funnel control under hard and soft output constraints, in: 2022 IEEE 61st Conference on Decision and Control (CDC), IEEE, 2022, pp. 4473–4478.

[40] R. Das, P. Jagtap, Prescribed-time reach-avoid-stay specifications for unknown systems: A spatiotemporal tubes approach, *IEEE Control Systems Letters* (2024).

[41] L. Sun, Y. Song, M. Lv, X. Huang, C. Wen, Event-triggered adaptive safe-oriented barrier lyapunov function-based boundary control of flexible beam systems characterized by uncertain euler–bernoulli pdes, *Automatica* 182 (2025) 112555.

[42] E. Restrepo, J. Matouš, K. Y. Pettersen, Tracking control of cooperative marine vehicles under hard and soft constraints, *IEEE Transactions on Control of Network Systems* (2024).

[43] B. S. Park, S. J. Yoo, Collision-free flexible performance tracking control against moving obstacles for underactuated surface vehicles with model uncertainty and input saturation, *Ocean Engineering* 288 (2023) 115968.

[44] S. J. Yoo, B. S. Park, Adaptive flexible performance function approach for dynamic obstacle avoidance to distributed formation tracking of range-constrained switched nonlinear multiagent systems, *International Journal of Robust and Nonlinear Control* 34 (7) (2024) 4864–4880.

[45] Y. Gilpin, V. Kurtz, H. Lin, A smooth robustness measure of signal temporal logic for symbolic control, *IEEE Control Systems Letters* 5 (1) (2020) 241–246.

[46] L. Grippo, M. Sciandrone, *Introduction to Methods for Nonlinear Optimization*, Springer, 2023.

[47] S. K. Mishra, G. Giorgi, *Invexity and optimization*, Vol. 88, Springer Science & Business Media, 2008.

[48] A. Wiltz, D. V. Dimarogonas, Handling disjunctions in signal temporal logic based control through non-smooth barrier functions, in: 2022 IEEE 61st Conference on Decision and Control (CDC), IEEE, 2022, pp. 3237–3242.

[49] T. G. Molnar, A. D. Ames, Composing control barrier functions for complex safety specifications, *IEEE Control Systems Letters* (2023).

[50] X. Cai, M. De Queiroz, Adaptive rigidity-based formation control for multirobotic vehicles with dynamics, *IEEE Transactions on Control Systems Technology* 23 (1) (2014) 389–396.

[51] M. W. Spong, S. Hutchinson, M. Vidyasagar, *Robot modeling and control*, John Wiley & Sons, 2020.

[52] E. D. Sontag, *Mathematical control theory: deterministic finite dimensional systems*, Springer-Verlag New York, Inc., 1998.

[53] H. K. Khalil, *Nonlinear Systems*, 3rd Edition, Prentice-Hall, New Jersey, 2002.